DESIGN OF BED PROTECTIONS; STABILITY AND MOVEMENT OF COBBLES, BOULDERS AND ROCKS

**by L.C. van Rijn (**www.leovanrijn-sediment.com**)**

Content
1. Introduction
2. Critical velocity and bed shear stress for coarse materials
3. Bed load transport of coarse materials
4. Conclusions

1.   Introduction

Cobbles, boulders and rocks are often used as a protection layer near a structure to cover the underlying sand bed against erosion by combined currents and waves.
Examples are: (1) rock protection around monopiles of windmills (see **Figure 1.1**); (2) cobble revetment at the upper beach; (3) rock protection as berth protection near harbour quay walls against ship propeller scour and (4) rock covers of pipelines against the impact of anchors and/or other objects.
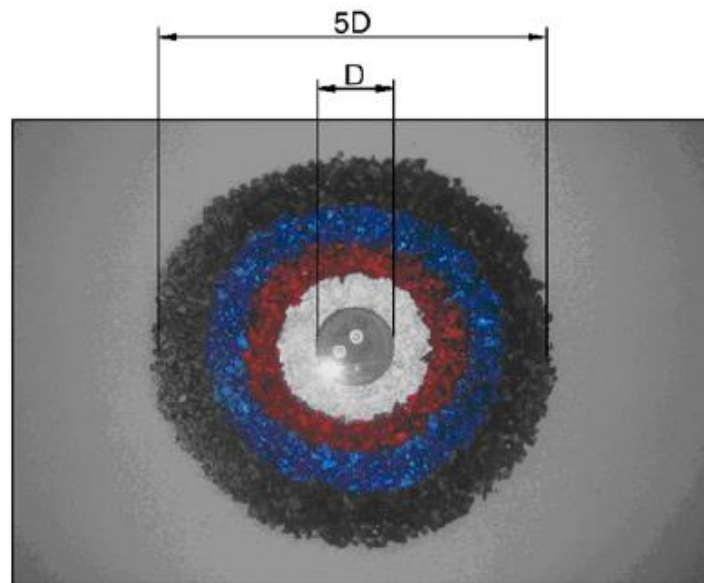
Figure 1.1   *Bed protection layer near a monopile of a windmill (De Vos et al., 2012)*

The design of a bed protection layer requires knowledge of the stability and movement (as bed load) of very coarse sediment materials. If some movement (or damage) is acceptable, the rock diameter can be designed to be smaller. This approach requires the inclusion of a damage level or damage parameter, which can be derived from the bed load equation of Paintal (1971) or Cheng (2002), which are both valid for relatively small Shields mobility numbers.

This note addresses the stability and movement of very coarse materials (cobbles, boulders and rocks) based on the concept of the critical Shields mobility number related to a prescibed damage level.

2. Critical velocity and bed-shear stress for coarse materials

2.1 Introduction

The stability of cobbles, boulders and rocks on a horizontal or a mild sloping bottom in a current with and without waves can be described by the method of Shields (Shields' curve) for granular material. This method is also known as the critical shear stress method. A drawback of this method is that the value of the friction coefficient is required which introduces additional uncertainty.

2.2 Critical shear-stress method

2.2.1 Shields mobility parameter

The problem of initiation of motion of granular materials due to a flow of water (without waves) has been studied by Shields (1936). Based on theoretical work of the forces acting at a spherical particle (see **Figure 2.2.1**) and experimental work with granular materials in flumes, he proposed the classical Shields' curve for granular materials in a current.
The Shields' curve expresses the critical dimensionless shear stress also known as the critical mobility number (θ_{cr}) as function of a dimensionless Reynolds' number for the particle, as follows:

$$\theta_{cr} = \tau_{b,cr}/[(\rho_s - \rho_w) \, g \, D_{50}] = \text{function } (u_{*,cr} \, D_{50}/\nu) \tag{2.2.1}$$

with:
$\tau_{b,cr} = \rho_w (u_{*,cr})^2$ = critical bed-shear stress at initiation of motion, $u_{*,cr}$= critical bed-shear velocity, ρ_s = density of granular material (2700 kg/m^3), ρ_w = density of water (fresh or saline water), ν= kinematic viscosity coefficient of water (=0.000001 m^2/s for water of 20 degrees Celsius), D_{50} = representative diameter of granular material based on sieve curve (Shields used rounded granular materials in the range of 0.2 to 10 mm; stones and rocks are represented by $D_{n,50}$ based on the particle volume).

The Shields' curve is shown in **Figure 2.2.1** and represents the transition from a state of stability to instability of granular material.
Granular material is stable if:

$$\theta \le \theta_{cr} \quad \text{or} \quad \tau_b/[(\rho_s - \rho_w) \, g \, D_{50}] \le \theta_{cr} \tag{2.2.2}$$

Based on detailed analysis of the data of existing research papers on the inititiation of fine cohesionless sediment particles in the range of 10 to 400 μm in the laminar and the tubulent flow range and the work of Soulsby (1997) and Van Rijn (1993), the following equation for the critical bed-shear stress related to initiation of motion is proposed:

$$\theta_{cr,shields}= 0.3/(1+D_*) + 0.055 \, [1-\exp(-0.02D_*)] \qquad \text{for } D_* > 0.1 \tag{2.2.3}$$

The θ_{cr}-value according to Shields-curve (solid black curve of **Figure 2.2.1**) is approximately constant at $\theta_{cr,shields} \cong 0.05$ (independent of the Reynolds' number; right part of Shields' curve) for coarse grains > 10 mm or $u_*D_{50}/\nu > 100$.
The precise definition of initiation of motion used by Shields is not very clear. Experimental research at Deltares (1972) based on visual observations shows that the Shields'curve actually represents a state with frequent movement of particles at many locations (p_m= percentage of moving particles is about 100%), see **Figure 2.2.1**. Hence, the Shields' curve cannot really be used to determine the critical stability of a particle.

The reduction parameter (r) from the relationship $\theta_{cr} = r\,\theta_{cr,shields}$ can be seen as a correction parameter acting on the Shields curve to define a particular stage of movement (or damage). Based on visual observations during initiation of motion experiments of Deltares (Deltares 1972; see Van Rijn 1993), the r-parameter is herein defined, as follows:

    r= 0.4 (occasional particle movement at some locations; $\cong$0.1% of surface is moving); damage level 1
        with minimum movement;
    r= 0.6 (frequent particle movement at some locations; $\cong$1% of surface is moving); damage level 2
        with very limited movement;
    r= 0.8 (frequent particle movement at many locations; $\cong$10% of surface is moving); damage level 3
        with some movement;
    r= 1.0 (frequent particle movement at nearly all locations; $\cong$50% of surface is moving; Shields' curve);
   damage level 5 with failure.

- measured
1 occasional particle movement at some locations
2 frequent particle movement at some locations
3 frequent particle movement at many locations
4 frequent particle movement at nearly all locations
5 frequent particle movement at all locations
6 permanent particle movement at all locations
7 general transport (initiation of ripples)
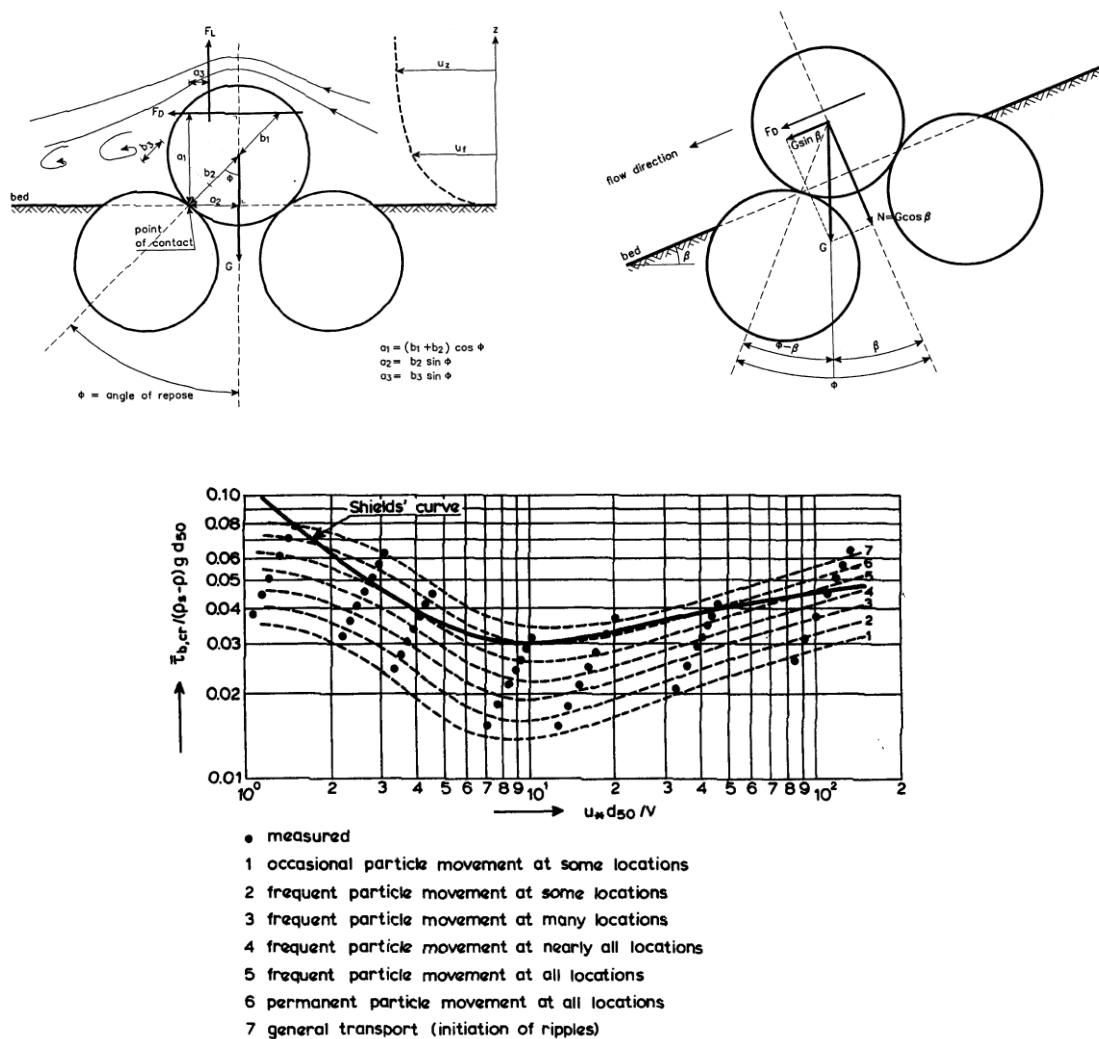
Figure 2.2.1   *Initiation of motion and Shields curve*

Van Rijn (1993) has shown that the Shields curve is also valid for conditions with currents plus waves, provided that the bed-shear stress due to currents and waves ($\tau_{b,cw}$) is computed as:

$$\tau_{b,cw} = \tau_{b,c} + \tau_{b,w} \tag{2.2.4}$$

with:

$\tau_{b,c}$ = $1/8\,\rho_w\,f_c\,\overline{u}^2$= bed-shear stress due to current (N/m²);

$\tau_{b,w}$ = $1/4\,\rho_w\,f_w\,\hat{U}^2$= bed-shear stress due to current (N/m²);

$\overline{u}$ = depth-mean current velocity (m/s);

$\hat{U}$ = near-bed peak orbital velocity (m/s) = $\pi H_s (T_p)^{-1} [\sinh(2\pi h/L_s)]^{-1}$ (linear wave theory);

f_c = $0.24[\log(12h/k_s)]^{-2}$; $f_{c,approx} \cong 0.11(h/k_s)^{-0.3}$ = current-related friction factor (-);

f_w = $\exp\{-6 + 5.2(\hat{A}/k_s)^{-0.19}\}$; $f_{w,approx} = 0.1(\hat{A}/k_s)^{-0.3}$ = wave-related friction factor (-);

h = water depth (m); H_s= significant wave height (m); L_s= significant wave length (m);

T_p = wave period of peak of wave spectrum (s);

$\hat{A}$ = $(T_p/2\pi)\hat{U}$ = near-bed peak orbital amplitude;

k_s = effective bed roughness of Nikuradse; (k_s= D_{max} with D_{max}= $\alpha D_{n,50}$ and α= 1 to 2 for narrow graded stones/rocks).

Using the Shields concept, the friction factors have to be known. The commonly used friction factors f_c and f_w are not practical. Therefore, approximate power functions $f_{c,approx}$ and $f_{w,approx}$ are introduced to simplify the computational methods.

The relative roughness parameters ($h/(\alpha D_{50})$; $\hat{A}/(\alpha D_{50})$) are in the range of 10 to 300 for coarse materials. **Table 2.2.1** shows the current-related and wave-related friction factors for relative roughness values in the range of 10 to 300 using the traditional methods and the new approximation methods. The current-related approximation function $f_{c,approx}$ is quite accurate, but the wave-related approximation function $f_{w,approx}$ is less accurate. This latter function can be much better represented by the function $f_{w,approx}=0.2[\hat{A}/(\alpha D_{50})]^{-0.5}$. However, if approximation functions with different powers are used, an explicit equation for the prediction of a stable value of $D_{n,50}$ cannot be obtained for combined curent+wave conditions. Therefore, fairly conservative approximation functions with an equal power of -0.3 have been used to obtain an explicit equation for the stable value of $D_{n,50}$ in combined current+wave conditions.

Relative roughness $h/(\alpha D_{50})$; $\hat{A}/(\alpha D_{50})$ (-)	Current-related friction			Wave-related friction	
	Chézy coefficient C=18log(12h/(αD_{50})) (m$^{0.5}$/s)	friction factor f_c=8g/C^2 (-)	approximate friction factor $f_{c,approx}$ =0.11[h/(αD_{50})]$^{-0.3}$ (-)	friction factor f_w (-)	approximate friction factor $f_{w,approx}$=0.1[$\hat{A}$ /(αD_{50})]$^{-0.3}$ (-)
10	37.4	0.056	0.055	0.071	0.050
15	40.6	0.048	0.049	0.055	0.044
20	42.8	0.043	0.045	0.047	0.041
50	50.0	0.031	0.034	0.029	0.031
100	55.4	0.026	0.028	0.022	0.025
150	58.6	0.023	0.024	0.018	0.022
200	60.8	0.021	0.022	0.017	0.020
300	64.1	0.02	0.020	0.014	0.018

Table 2.2.1 *Current-related and wave-related friction factors*

2.2.2 Slope effects

In the case of a mild sloping bed (**Figure 2.2.1**; Van Rijn 1993) the θ_{cr}-value can be computed as:

$$\theta_{cr} = K_{\alpha 1} K_{\alpha 2} r \theta_{cr,shields} \tag{2.2.5}$$

with:

K_{slope1} = $\sin(\phi-\alpha_1)/\sin(\phi)$ = slope factor for upsloping velocity; $\sin(\phi+\alpha_1)/\sin(\phi)$ for upsloping velocity;

K_{slope2} = $[\cos(\alpha_2)][1 - \{\tan(\alpha_2)\}^2/\{\tan(\phi)\}^2]^{0.5}$ = slope factor for longitudinal velocity;

r = reduction parameter (damage parameter);

$\theta_{cr,shields}$= critical Shields' number at horizontal bottom (Equation 2.2.3);

α_1 = angle of slope normal to flow or wave direction (slope smaller than 1 to 5);

α_2 = angle of slope parallel to flow or waves (slope smaller than 1 to 3);

ϕ = angle of repose (30 to 40 degrees).

2.3 Stability and damage equations for coarse materials in currents

2.3.1 Equations

Using the available formulae (2.2.4 and 2.2.5) and $\tau_{b,c} = 1/8 \, \rho_w \, f_c \, \overline{u}^2$; $f_{c,approx} \cong 0.11[h/(\alpha D_{n,50})]^{-0.3}$ for large rocks; $\theta_{cr} = r\theta_{cr,shields}$, and $\tau_{b,c} = \theta_{cr} \, (\rho_s - \rho_w) \, g \, D_{n,50}$; the critical diameter can be expressed as:

$$D_{n,50} = \gamma_s \, [(s-1) \, g \, K_{\alpha1} \, K_{\alpha2} \, r \, \theta_{cr,shields}]^{-1.4} \, [0.013 \, (h/\alpha)^{-0.3} \, (\gamma_{str} \, \overline{u})^2]^{1.4} \qquad (2.3.1)$$

with:
r = reduction factor (0.5 to 1),s= ρ_s/ρ_w,h= water depth, $\overline{u}$ = depth-mean velocity,
$K_{\alpha1}$ = slope factor for longitudinal slopes, $K_{\alpha2}$ = slope factor for lateral slopes,
$\theta_{cr,shields}$= critical Shields mobility parameter based on Equation 2.2.3; ($\theta_{cr,shields} \cong 0.05$ for coarse materials),
α = bed roughness coefficient ($k_s = \alpha D_{n,50}$ with α=1 to 2),
γ_s = safety factor and γ_{str}= velocity+turbulence enhancement factor due to the presence of structures such as bridge piles or windmill piles (γ_{str}=1.2 to 1.5); γ_{str} =1 to 1.2 if velocity enhancement is caused by the protruding bed protection itself without the presence of an upstream structure).

2.3.2 Field and flume data of critical velocity and bed-shear stress of rocks and boulders

Most of the research on initiation of motion of particles is related to relatively small size particles with diameters < 10 mm (see Shields 1936, Graf 1971, Yalin 1977, Van Rijn 1993, Soulsby 1997) and will not be discussed here. In this paper, the attention is focused on critical conditions of large size pebbles, cobbles, boulders and rocks in the laboratory and at various field sites.
Helley (1969) has studied the threshold velocities of large size rocks (0.15 to 0.45 m) in the Blue Creek mountain river in the USA. Thirty-six natural rocks of various sizes and shapes were painted fluorescent red, tagged by a float and placed in a study reach in the Blue Creek (summer and fall of 1967) where near-bed velocities could be measured close to the tagged rocks. The water depth was in the range of 1 to 1.2 m. Initiation of motion was defined as the sudden movement of the floats. Helley also presents the field data of similar measurements by Fahnestock (1963), see **Table 2.3.1**.
Inbar and Schick (1979) have studied the critical movement of boulders and rocks during flash floods in the upper Jordan River and the Meshushim River in Israel (see also **Section 3.2.2**).
An extreme rainstorm (once in 100 years) in January 1969 generated a flood in the Jordan River. Boulders up to 1.3 m were moved, and the channel was completely reshaped. During the same event, a 300 m^3/s peak flow occurred in the neighboring Nahal Meshushim River. Here too, numerous boulders of 1 m were transported. The critical flow velocities in depths of 1 to 1.5 m can be summarized, as follows: $u_{critical}$= 2-2.5 m/s, for D_{50}= 0.25-0.5 m and $u_{critical}$= 2.5-3 m/s for D_{50}= 0.5-1 m, see **Table 2.3.1**.
Turowski et al. (2009) have studied the movement of boulders and rocks in the Erlenbach mountain stream; a small stream with step-pool morphology in the canton of Schwyz, Switzerland. Three exceptional events have occurred and partly or completely rearranged the existing step-pool morphology. In the aftermath of the events, sediment transport rates at a given discharge and total sediment yield remained at higher values for about a year or longer. For the last event, dated on the 20 June 2007, observations of boulder mobility and step destruction were used to interpret channel stability. Boulders with median diameters of up to 1.35 m and estimated weights of more than 2.5 tons have moved during the 2007 event. Boulders of about 0.5 to 0.65 m were found to have been fully mobile in peak conditions with mean velocities of about 3 m/s (discharge of about 15 m^3/s, mean flow width of 4 m and mean flow depth of 1.2 m).
Mueller et al. (2005) have studied the threshold bed-shear stress (θ_{cr}) of bed-load transport of rocks and boulders with D_{50}-values in the range of 0.025 to 0.21 m in various mountain streams (Idaho, USA). The θ_{cr}-value is defined as the dimensionless bed-shear stress at a very low dimensionless reference bed-load transport rate of 0.002. The reference transport rate is assumed to represent flow conditions that are just high enough to begin mobilizing sediment from the bed surface. A typical phenomenon of mountain streams

5

is the wide grain-size distribution including patches of finer, more mobile sediment and large, relatively immobile boulders that are often arranged into cascades or steps. Annual snowmelt and stormflows can mobilize fine sediment while boulders only move in rare, larger floods or debris flows. The large, relatively immobile grains disrupt the flow and increase turbulence.

Figures 2.3.1, 2.3.2 and **2.3.3** show the θ_{cr}-values as function of the size D_{50}, the ratio D_{50}/D_{90} and the ratio h/D_{50}. The critical Shields-parameter varies considerably in the range of 0.01 to 0.12. Hence, the lowest values are much smaller than the Shields-curve values (**Figure 2.2.1**), which means that cobble/boulder/rock movement is possible at very low mobility values of 0.01 to 0.02.

The mean value of all values is about 0.047 (as used in the Meyer-Peter-Mueller 1948-formula). The larger rocks may have a smaller θ_{cr}-value of about 0.03 to 0.04. The ratio D_{50}/D_{90} has a clear effect on the θ_{cr}-value. This ratio expresses the grading of the bed material; a small value means a wide grading resulting in hiding-exposure effects. Smaller rocks/fragments are more difficult to mobilize, as they are hiding between the larger rocks. Uniform cobbles have a smaller θ_{cr}-value. Rocks are also more difficult to move in the case of small submergence (h/D_{50} is small), because the flow resistance is relatively large and the near-bed velocities are relatively small. Flow resistance typically increases as relative submergence decreases and streams become steeper, smaller, and coarser. Large, relatively immobile grains cause local accelerations and decelerations in the flow, hydraulic jumps, large vertical velocities, localized intense turbulence, and areas of eddying water with weak net flow.
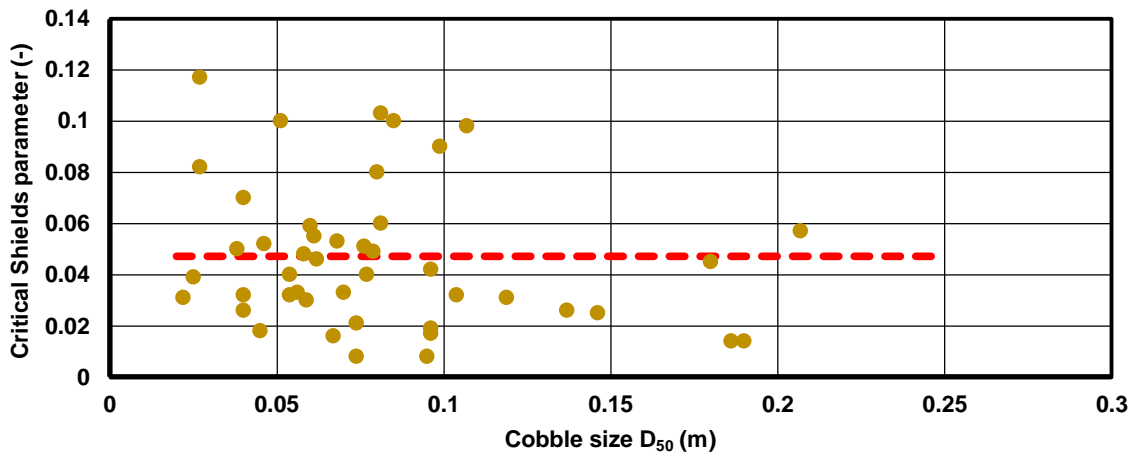

Figure 2.3.1 *Critical Shields parameter (θ_{cr}) as function of D_{50}*
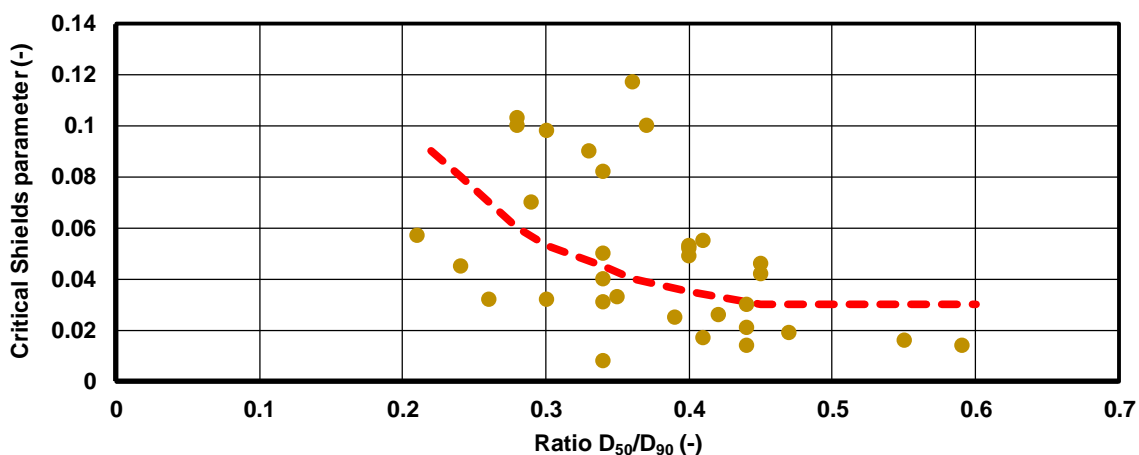

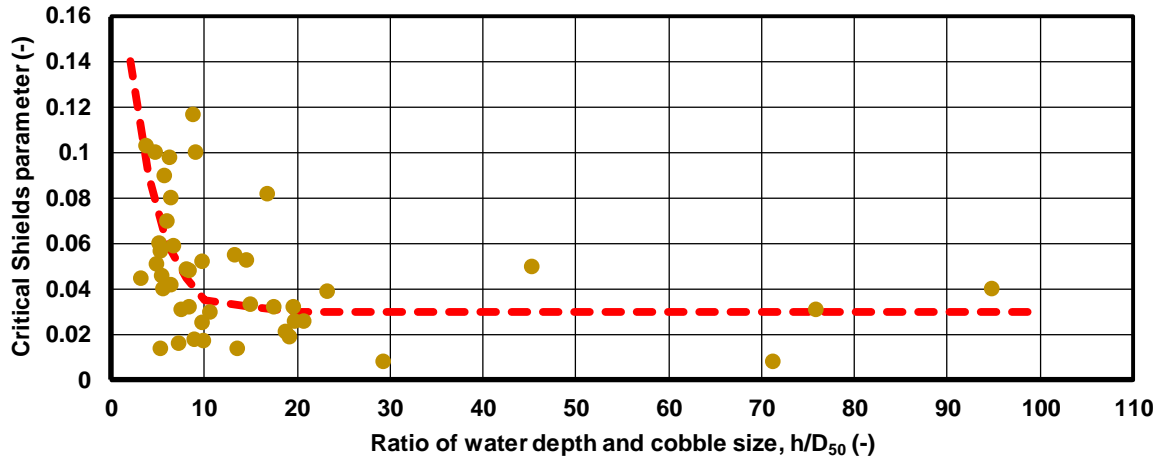**Figure 2.3.2** *Critical Shields parameter (θ_{cr}) as function of the ratio D_{50}/D_{90}*

Figure 2.3.3 *Critical Shields parameter (θ_{cr}) as function of the ratio h/D_{50}*

Atal and Lavé (2009) have studied the movement of pebbles and rocks with diameters in the range of 5 to 80 mm in a circular flume. Particle trajectories and collisions were recorded and analyzed using a high-speed camera. Pebbles moved by saltation and occasionally by rolling. Mean saltation velocities during the saltations (hops) were measured directly from particle tracking on the movies. **Figure 2.3.4** shows the particle velocity as function of the fluid velocity.

The particle velocity can be expressed as $u_{particle} \cong 0.7\ u_{fluid}$. The critical velocities are roughly: $u_{critical}$= 1 m/s for D_{50}= 15 mm to $u_{critical}$= 1.75 m/s for D_{50}= 70 mm, see **Table 2.3.1**.
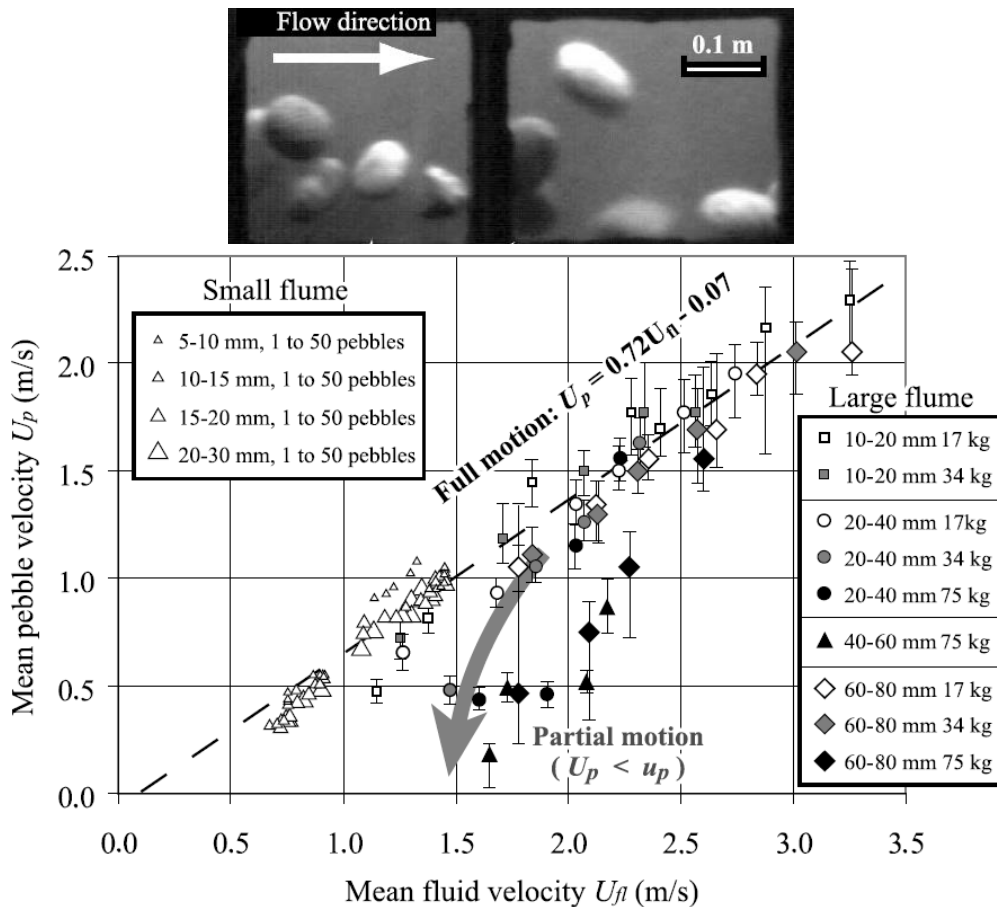

Figure 2.3.4   *Mean velocity of pebbles as function of the fluid velocity in the flume*
(full motion= continuous motion; partial motion= motion including resting periods)

Summary of results

All data are summarized in **Table 2.3.1** and in **Figure 2.3.5**. The uncertainty range of particle size and critical velocity is about 10% for the flume data and 15% to 20% for the field data. It is noted that the field data with large rock sizes up to 0.7 m refer to very shallow mountain rivers with depths in the range of 0.5 to 1.2 m ($h/D_{50}<10$). This type of flow is generally known as the "wild" water regime with exceptionally high turbulence levels exceeding those of normal open channel flow ($h/D_{50}>100$). Furthermore, the field data tests of relatively large rocks concern the initiation of motion of very isolated rocks which are placed on top of the river bed and are thus extremely exposed to the local turbulent velocities. This test arrangement is very different from a bed protection layer consisting of rocks of approximately the same size with sheltering effects due to the presence of neighbouring rocks.

Equation (2.3.1) has three input parameters: α-coefficient related to bed-roughness effect (range 1 to 2), r-coefficient related to the most appropriate critical Shields mobility number range (range 0.3 to 0.6) and the γ_{str}-coefficient related to the velocity and turbulence enhancement due to the bed-structure arrangement (range 1 to 1.5). The α-coefficient is set to $\alpha=2$, which means that the effective bed roughness is equal to $k_s=2D_{50}\cong1D_{90}$. The other two coefficients have been calibrated using the data of **Figure 2.2.6**. Computed results are shown for r=0.3, 0.4 and 0.5 and $\gamma_{str}=1.2$. This latter coefficient represents the effect that the rocks used in de field tests are isolated rocks fully exposed to the flow with extreme turbulence levels. Fairly good agreement between measured and computed results can be observed for r=0.4 and r=0.5 in combination with $\gamma_{str}=1.2$.
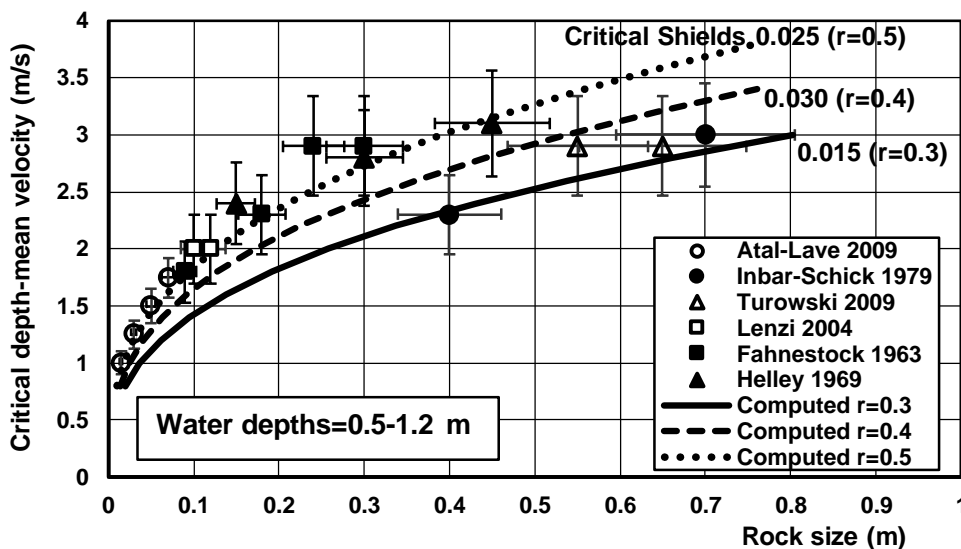
Figure 2.3.5 *Critical depth-mean velocity as function of rock size in currents ($\gamma_{str}=1.2$)*

Data set	Water depth (m)	Particle/rock size (m)	Critical depth-mean velocity (m/s)
Flume: Atal and Lavé 2009	<0.5	0.015; 0.03; 0.05; 0.07	1.0; 1.25; 1.5; 1.75
Field: Inbar and Schick 1979	1-1.2	0.4; 0.7	2.3; 3.0
Field: Turowski et al. 2009	0.5-1	0.6	3.0
Field: Lenzi 2004, Lenzi et al. 2006, Mao and Lenzi 2007, Rainato et al. 2017	<0.5	0.11	2.0
Field: Fahnestock 1963	0.5-1	0.09; 0.18; 0.24; 0.3	1.8; 2.3; 2.9; 2.9
Field: Helley 1969	1-1.2	0.15; 0.3; 0.45	2.4; 2.8; 3.1

Table 2.3.1 *Summary of critical conditions for large size particles/rocks in current conditions*

2.3.3 Damage estimate

A damage estimate can be obtained if the bed load transport at low mobility parameters in the range of 0.01 to 0.05 can be computed.

An important contribution to the study of the stability of granular material has been made by Paintal (1971), who has measured the dimensionless (bed load) transport of granular material at conditions with θ-values in the range of 0.01 to 0.05, see **Table 2.3.2** (and also **Figure 3.2.2**). Paintall (1971) and later Cheng (2002) have used measured bed load transport data to derive fairly simple bed load transport equations.

Using the approach of Paintal (1971) or Cheng (2002), the bed load tranport of granular material at very small θ-values can be computed by (see Chapter 3):

Paintal (1971): $\Phi_b = 6.6 \; 10^{18} \; \theta^{16}$ (2.3.2a)

$q_b = 6.6 \; 10^{18} \; \theta^{16} \; \rho_s \; \{(s-1)g\}^{0.5} (D_{50})^{1.5}$

or

Cheng (2002): $\Phi_b = 13 \; \theta^{1.5} \exp(-0.05/\theta^{1.5})$ (2.3.2b)

$q_b = 13\theta^{1.5}\exp(-0.05/\theta^{1.5}) \; \rho_s \; \{(s-1)g\}^{0.5} (D_{50})^{1.5}$

with:

Φ_b $= (\rho_s)^{-1} \{(s-1)g\}^{-0.5} (D_{50})^{-1.5} q_b$;

q_b = bed load transport by mass (kg/m/s);

θ $= \tau_b/[(\rho_s - \rho_w) g D_{50}]$ = dimensionless bed-shear stress (Shields number);

s $= \rho_s/\rho_w$ = relative density;

τ_b = bed-shear stress due to current (N/m^2).

θ-values	Dimensionless bed load transport Φ measured by Paintal (1971)
0.02	$4.3 \; 10^{-9}$
0.025	$1.5 \; 10^{-7}$
0.03	$3. \; 10^{-6}$
0.04	$3. \; 10^{-4}$

Table 2.3.2 *Bed load transport values measured by Paintal (1971)*

The bed load transport (q_b) is given in kg/m/s, which can be converted into the number of moving rocks per unit width (m) and time (s) by using the mass of one rock $M_{rock} = (1/6) \; \pi \; \rho_s \; D_{50}^3$ resulting in:

Paintal (1971): $N_{moving \; rocks} = \gamma_s \; [6.6 \; 10^{18} \; \theta^{16} \; \rho_s \; \{(s-1)g\}^{0.5} (D_{50})^{1.5}]/[(1/6) \; \pi \; \rho_s \; D_{50}^3]$

$N_{moving \; rocks} = \gamma_s \; [13 \; 10^{18} \; \theta^{16} \; \{(s-1)g\}^{0.5} (D_{50})^{-1.5}]$ (2.3.3a)

Cheng (2002): $N_{moving \; rocks} = \gamma_s \; [13 \; \theta^{1.5} \exp(-0.05/\theta^{1.5}) \; \rho_s \; \{(s-1) g\}^{0.5} (D_{50})^{1.5}]/[(1/6) \; \pi \; \rho_s \; D_{50}^3]$

$N_{moving \; rocks} = \gamma_s \; [25 \; (r\theta_{cr,shields})^{1.5} \exp\{-0.05/(r\theta_{cr,shields})^{1.5}\} \{(s-1) g\}^{0.5} (D_{50})^{-1.5}]$ (2.3.3b)

with:

$N_{moving \; rocks}$ = number of moving rocks per m and per s (per day by multiplication with 86400 s);

Δt = time period (in s; 1 day=86400 s);

θ = mobility parameter;

γ_s = safety factor.

Equation (2.3.3b) is implemented in the **ARMOUR.xls** model.

Equation (2.3.3) can be related to the damage parameter $S_d = A_e/D_{n,50}^2$, as follows:

$S_d = A_e/(D_{n,50})^2 = \Delta t\, N_{movingrocks}\, V_{1rock}/(D_{n,50})^2 = 0.5\, \Delta t\, N_{movingrocks}\, (\pi/6)\, (D_{n,50})^3/(D_{n,50})^2 \cong 0.5\, \Delta t\, N_{movingrocks}\, D_{n,50}$

with: A_e= eroded area per unit width in time period Δt; V_{1rock} = volume of a single rock; Δt= time period considered (usually 5000 to 10000 waves or about 1 day of storm).

The number of rocks moving out of the bed protection area in a given time period can be seen as damage requiring maintenance. The damage percentage in a given time period can be computed as the ratio of the number of rocks moving away and the total number of rocks available.

The loss of rocks from a bed protection area with length L and thickness $\delta_{bp} = \alpha_{bp} D_{n,50}$ can be determined, as follow:

Volume of bed protection per unit width: $V_{bp} = L_{bp}\, \delta_{bp}$

Number of rocks in bed protection area: $N_{rocks,bp} = (1-\varepsilon)L_{bp}\, \alpha_{bp}D_{n,50}/\{(\pi/6)D_{n,50}^3)\} = (6\alpha_{bp}/\pi)\, (1-\varepsilon)\, L_{bp}\, (D_{n,50})^{-2}$.

Number of rocks moving out of bed protection area during the lifetime: $N_{rock,out} = N_{moving\ rocks}\, T_{extreme\ event}\, T_{life}$.

The Loss coefficient is:

$\qquad P_{Loss} = [N_{moving\ rocks}\, T_{extreme\ event}\, T_{life}]/N_{rocks,bp} = [N_{moving\ rocks}\, T_{extreme\ event}\, T_{life}]/\, [2\alpha_{bp}(1-\varepsilon)\, L_{bp}\, (D_{n,50})^{-2}]$ $\qquad$ (2.3.4)

with:

L_{bp}= length of bed protection area (normal to flow or waves);

$\delta_{bp} = \alpha_{bp}D_{n,50}$ = thickness of bed protection ($\alpha \cong$ 2 to 3);

ε = porosity of bed protection layer ($\cong$0.45);

$T_{extreme\ event}$= duration of extreme events per year (in days per year); storm event or river flood event;

T_{life}= lifetime of structure (in years);

$N_{moving\ rocks}$= number of rocks moving out of bed protection area (per unit width and per day).

Figure 2.3.6 shows the number of moving rocks (per m width and per day; Δt=86400 s) based on the Cheng-equation (2.3.3b) for an example case with rocks in the range of D= 0.02 to 0.5 m and current velocities in the range of 1 to 7 m/s. The water depth= 5 m. The input parameters are α=2, γ_{str}=1, τ_b= 1/8 $f_c\ \overline{u}$ and $\theta = \tau_b/[(\rho_s-\rho)\, g\, D]$.

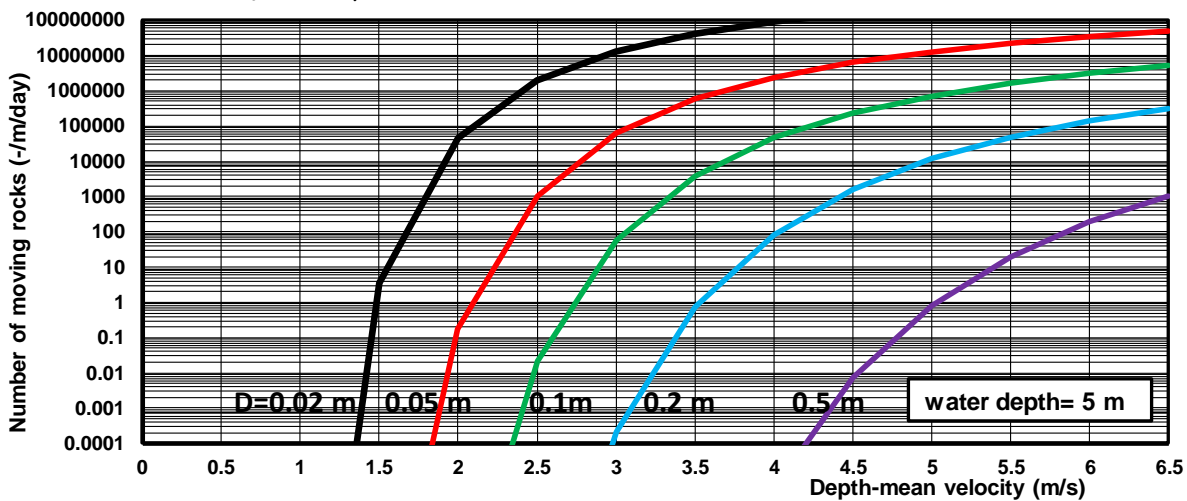Assuming almost no movement for $N_{rocks} < 0.0001$ (per m and per day), the critical depth-mean velocities are:

$\qquad$ D=0.02 m: $\quad \overline{u}_{cr} \cong$ 1.3 m/s,

$\qquad$ D=0.05 m: $\quad \overline{u}_{cr} \cong$ 1.8 m/s,

$\qquad$ D=0.1 m: $\quad\ \overline{u}_{cr} \cong$ 2.3 m/s,

$\qquad$ D=0.2 m: $\quad\ \overline{u}_{cr} \cong$ 3.0 m/s,

$\qquad$ D=0.5 m: $\quad\ \overline{u}_{cr} \cong$ 4.2 m/s.

Figure 2.3.6 *Number of moving rocks of horizontal bed protection in current conditions (h= 5 m)*

2.3.4 Practical applications bed protection

Equation (2.3.1) has been used to produce a design graph for horizontal bed protections in water depths of h_o= 3 to 20 m and depth-mean velocities u_{mean}= 1 and 5 m/s. The thickness of the protection layer is set to δ_{bp}= 0.5 m. The effective water depth is: $h_{bp}=h_o-\delta_{bp}$.

Other parameters are: density seawater= 1020 kg/m³; density sediment= 2650 kg/m³; α=2, $\theta_{cr,o}$= r $\theta_{cr,shields}$ with r= 0.5 and $\theta_{cr,shields}$ = 0.05; γ_{str} = 1 (no additional velocity-turbulence enhancement due to bed protection layer) and γ_s =safety factor= 1. The computed results are shown in **Figure 2.3.7**.

The results clearly show that the rock diameter decreases for increasing water depth at the same depth-mean velocity, because the bed-shear stress decreases with increasing water depth (less flow resistance).

In the case of a bed protection with rock size=D_{50}=0.1 m, thickness δ_{bp}=0.5 m, $\alpha_{bp}=\delta_{bp}/D_{50}$=5, length L_{bp}= 50 m, porosity ε= 0.45 in a flow with depth of h=5 m and current velocity u=2.5 m/s (during 30 days per year), the number of moving rocks is N_{mr}=0.02 (**Figure 2.3.6**) with S_d= 0.001.

The loss coefficient of rocks for the lifetime (50 years) of the bed protection layer is:

P_{Loss}= [0.02x30x50]/[2x5x(1-0.45)x50x(0.1)$^{-2}$]= 30/27500= 0.0011 (0.11%) during the lifetime of the stucture. The thickness of the protection layer can be reduced to 0.3 m resulting in a loss coefficient of about 0.2%.

In both cases (δ_{bp}=0.5 m or 0.3 m), the damage is so low that a static bed protection is obtained.

Using: rock size=D_{50}=0.08 m and δ_{bp}=0.5 m, the number of moving rocks per m per day goes up to N_{mr}=1 (50 times larger, Figure 2.3.6) and S_d=0.04. The loss coefficient goes up by a factor of 50 to about 6%, which may be acceptable (dynamic bed protection for a smaller rock size D_{50}=0.08 m).
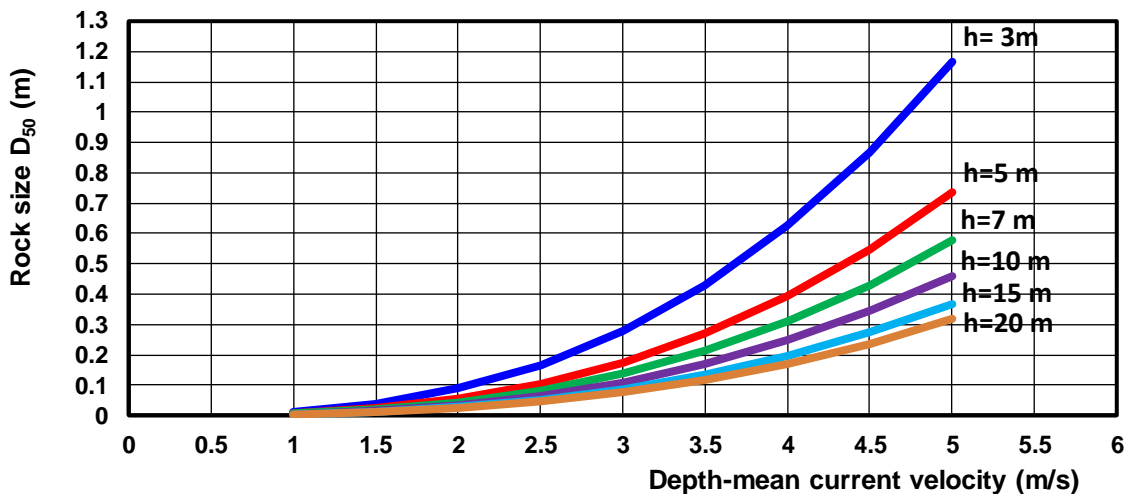

Figure 2.3.7 *Design graph (r= 0.5, γ_{str}= 1) for horizontal bed protection in current conditions*

2.4 Stability and damage equations for coarse materials in waves

2.4.1 Equations

Using the available formulae (2.2.3, 2.2.4 and 2.2.5) and $\tau_{b,w}$ = 1/4 ρ_w f_w $\hat{U}^2$, $f_{w,approx} \cong 0.1$ [$\hat{A}$ /($\alpha D_{n,50}$)]$^{-0.3}$ for large stones, $\hat{A}$ = $\hat{U}$ T_p/(2π)= orbital amplitude, $\tau_{b,c}$ = 0, θ_{cr}= r $\theta_{cr,shields}$ and $\tau_{b,w}$ = $\theta_{cr}(\rho_s-\rho_w)$ g $D_{n,50}$; the critical diameter can be expressed as:

$$D_{n,50} = \gamma_s \ [(s-1) \ g \ K_{\alpha 1} \ K_{\alpha 2} \ r \ \theta_{cr,shields}]^{-1.4} \ [0.045 \ (T_p/\alpha)^{-0.3} \ (\gamma_{str} \ \hat{U})^{1.7}]^{1.4} \qquad (2.4.1)$$

with:

r   = reduction factor; diameter decreases for increasing r between 0.5 and 1;

α = bed roughness coefficient (k_s= $\alpha D_{n,50}$ with α= 1.3 to 2); diameter increases for increasing α;

γ_s = safety factor; diameter increases for increasing γ_s;

γ_{str} = 1 to 1.5= velocity+turbulence enhancement factor due to the presence of a structure (bed protection around a monopile),

s = ρ_s/ρ_w, $K_{\alpha 1}$ = slope factor for longitudinal slopes, $K_{\alpha 2}$ = slope factor for lateral slopes,

$\theta_{cr,shields}$= critical Shields mobility parameter based on Equation 2.2.3; ($\theta_{cr,shields} \cong 0.05$ for coarse materials).

Equation (2.4.1) is implemented in the **ARMOUR.xls** model.
Equations (2.3.3b) can be used to get an estimate of the number of moving rocks (damage) during a given period (used in **ARMOUR.xls**).
The damage parameter $S_d = A_e/D_{n,50}^2$ can be estimated by:

$S_d = A_e/(D_{n,50})^2 = \Delta t\, N_{movingrocks}\, V_{1rock}/(D_{n,50})^2 = 0.5\, \Delta t\, N_{movingrocks}\, (\pi/6)\, (D_{n,50})^3/(D_{n,50})^2 \cong 0.5\, \Delta t\, N_{movingrocks}\, D_{n,50}$

with: A_e= eroded area per unit width in time period Δt; Δt= time period considered (usually 5000 to 10000 waves or about 1 day of storm) and $N_{movingrocks}$ = number of moving rocks per m width and second based on Equation (2.3.3b).

2.4.2 Field data of critical velocity

Crickmore et al. of HR Wallingford (1972) have performed a pebble tracer experiment in the English Channel east of Portsmouth in the period September 1969 to April 1971. The local seafloor consists of natural pebbles/shingle of flint material. The peak tidal velocities are 0.5 m/s during neap tide and 0.8 m/s during spring tide. Radioactive tagged pebbles (D=28 mm, D_{min}=19 mm, D_{max}=38 mm) were placed by divers at three areas (30x60 m²) with depths of 9, 12 and 18 m (about 1000 tagged pebbles at each area). The site is exposed to waves from south-west to south-east. Wave records were obtained at the Owers light vessel at a depth of about 25 m (about 25 km south-west from the pebble areas). Tracer displacement was measured by towing a detection instrument behind the survey vessel (4 surveys in the period september 1969 to April 1971). The inaccurary of the horizontal positioning system was estimated to be about 5 to 10 m. The thickness of the upper bed layer in which tagged particles were observed, was in the range of 60 to 120 mm. Various storms did occur during the observation period. The maximum significant wave height was about $H_{s,max}$= 5 m in depth of 18 m reducing to $H_{s,max}$=3 m in a depth in 9 m (wave period of about 8 to 10 s). The pebble movement was about 40 m at the site with depth of 9 m, about 15 m at a depth of 15 m and zero at a depth of 18 m.

Table 2.4.1 (Row 1) shows the measured results for the site with depth of 18 m. Based on this, the critical peak orbital velocity of pebbles with D_{50}= 0.028 m is estimated to be $\hat{U}_{cr} \cong 1.2$ m/s. Equation (2.4.1) yields $D_{n,50}$=0.028 m for r$\cong$ 0.7, s=2.6, γ_{str}=1 (no structure), T_p=8 s, α=2, see also **Figure 2.4.1**. This corresponds to a critical mobility number of $\theta_{cr} \cong 0.035$, which is much lower than the standard critical Shields value of $\theta_{cr,shields}$= 0.05.

Sediment size		Type of material	Density	Water depth	Estimated critical velocity for sliding and rolling
Range	Mean				
(m)	(m)		(kg/m³)	(m)	(m/s)
0.019-0.038	0.028	quartz	2650	9-18	1.2
0.14-0.27	0.2	agglomerate	2360	2-4	2.1
0.16-0.48	0.3	sandstone	2550	2-4	2.2
0.22-0.73	0.45	sandstone	2550	2-4	3.4
0.33-1.25	0.75	agglomerate	2360	2-4	3.7
0.8-1.15	1.0	basalt	3040	2-4	4.9
0.59-1.59	1.1	basalt	3040	2-4	5.5
1.07-2.1	1.5	sandstone	2550	2-4	5.7
0.74-2.51	1.6	basalt	3040	2-4	6.4
1.23-3.05	2.0	basalt	3040	2-4	6.9

Table 2.4.1 *Summary of critical conditions for large size particles/rocks in wave conditions*

Hall (2010) and Hansom et al. (2008) have studied the movement of natural boulders in conditions with breaking waves at the shore platform of East Lothian on the high-energy, macro-tidal North Sea coast of Scotland. Boulders with volumes of more than 0.5 m³ have been moved landward over extensive areas of the shore platform. Velocity in breaking waves are estimated to have reached values of 3 to 4 m/s on the platform, especially in the sligthly deeper channels eroded in the platform floor. Sliding is the dominant mechanism of movement for irregular shaped (mega) clasts. Rolling and overturning processes occur for platy clasts. Boulder sizes and estimated critical velocities related to boulder sliding are given in **Table 2.4.1** (row 2-10) and in **Figure 2.4.1**.
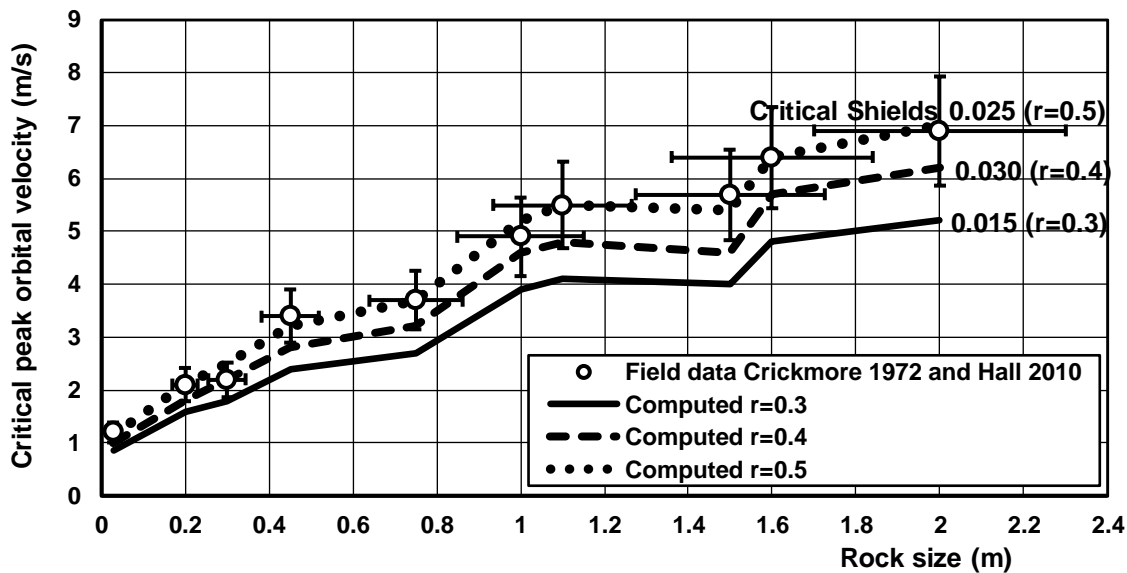
Figure 2.4.1 *Critical peak orbital velocity as function of rock size in waves (γ_{str}=1.2)*

Equation (2.4.1) has been used to compute the critical peak orbital velocity for the boulder sizes of **Table 2.4.1** using: ρ_w= 1020 kg/m³, α=1=bed roughness coefficient, r=Shields-reduction coefficient=0.3, 0.4 and 0.5 and γ_{str}=1.2= velocity enhancement coefficient. This latter coefficient represents the effect that the boulders at the field site are isolated rocks fully exposed to breaking waves with extreme turbulence levels.
Computed results are shown in **Figure 2.4.1** for r=0.3, 0.4 and 0.5 and γ_{str}=1.2. Fairly good agreement between measured and computed results can be observed for r= 0.4 and r=0.5 in combination with γ_{str}=1.2. These settings also yield the best results for rocks in currents (see **Figure 2.3.5**).

2.4.3 Practical application bed protection

Equation (2.4.1) has been used to produce a design graph for horizontal bed protections in water depths of h= 3 to 20 m and significant wave heights between H_s= 0.1 and 12 m. The wave period T_p is given by the relationship T_p= 5 $H_s^{0.4}$ (North Sea wave climate). The thickness of the protection layer is set to δ_{bp}= 0.5 m.
The effective water depth is h_{bp}=h_o-δ_{bp}. Other parameters are: density of seawater= 1020 kg/m³; density of sediment= 2650 kg/m³; γ_s=1= safety factor, γ_{str}=1, α=2, r= 0.5 and $\theta_{cr,shields}$ = 0.05. The computed results are shown in **Figure 2.4.2**.
For example: h=17 m and H_s= 4.6 m (T_p= 9.2 s) yields: $D_{n,50}$= 0.048 m for r= 0.5 and $N_{moving\ rocks}$= 10 rocks/m/day. This latter parameter can be reduced to N_{mr}=0.033 by using a smaller rock size $D_{n,50}$=0.066 m (r= 0.4).
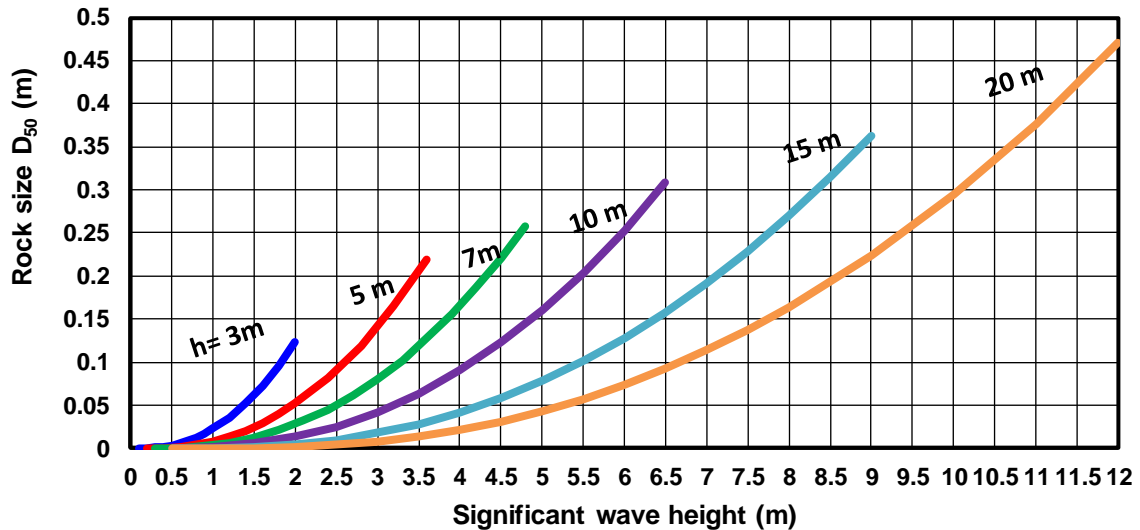
Figure 2.4.2 *Design graph (r= 0.5; γ_{str}=1) for horizontal bed protection in wave conditions*

2.4.4 Practical application toe protection

The toe structure of a breakwater provides support to the armour layer slope and protects the structure against damage due to scour. Most often, the toe consists of rubble mound of rocks/stones. Usually, the width of the toe varies in the range of 3 to 10 $D_{n,50}$ and the thickness of the toe varies in the range of 2 to 5 $D_{n,50}$ depending on the conditions, see **Figure 2.4.3**.
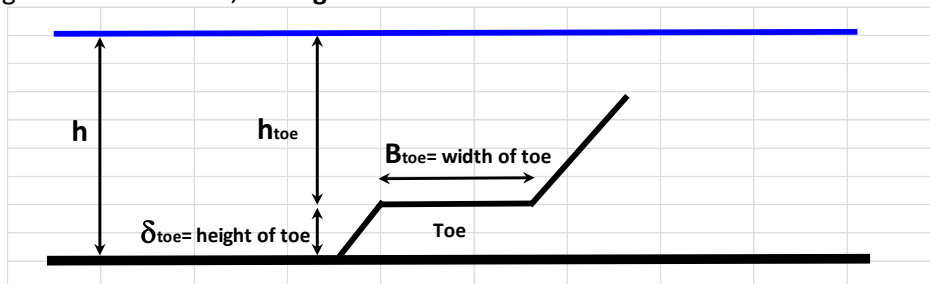

Figure 2.4.3 *Toe protection dimensions*

Based on laboratory tests in a wave flume, Van der Meer (1998) has proposed:

$$D_{n,50} = [6.2(h_{toe}/h)^{2.7} + 2] \, \Delta^{-1} \, N_{od}^{-0.15} \, H_{s,toe} \qquad \text{for } 0.4 < h_{toe}/h < 0.9 \qquad (2.4.2)$$

with: N_{od}= damage parameter (0.5-1 = start of damage; 2 = severe damage and 4 = failure).

Based on laboratory tests in a wave flume (non-overtopped rock slope of 1 to 2; permeable core; foreland of 1 to 30; no severe wave breaking at foreland), Van Gent and Van der Werf (2014) have proposed:

$$D_{n,50}= 0.32 \, [H_{s,toe}/(\Delta \, N_{od}^{0.33})] \, (B_{toe}/H_{s,toe})^{0.1} \, (\delta_{toe}/H_{s,toe})^{0.33} \, [U_{max}/(g \, H_{s,toe})^{0.5}]^{0.33} \qquad (2.4.3)$$

with: B_{toe} = width of toe; δ_{toe} = height of toe; N_{od}= damage parameter; $U_{max}= \pi \, H_{s,toe}/(T_{m-1,0} \sinh(kh_{toe}/L_o))$ = peak orbital velocity at toe based on deep water wave length; k= 2π/L = wave number; L_o = wave length at deep water = $(g/2\pi) \, (T_{m-1,0})^2$; h_{toe}= water depth above toe; h= water depth in front of toe; $\Delta=(\rho_s - \rho_w)/\rho_w$.

Equation (2.4.3) is valid for h_{toe}/h = 0.7 to 0.9 or δ_{toe}/h = 0.1 to 0.3. The peak orbital velocity (U_{max}) is based on the deep water wave length (L_o) which leads to relatively large U_{max}-values in shallow water and hence relatively large $D_{n,50}$-values for shallow depths.

Figure 2.4.4 shows the computed rock size for increasing depth above the toe protection based on Equations (2.4.1, 2.4.2 and 2.4.3). The variation of the peak orbital velocity is also shown (right axis). Equation (2.4.3) of Van Gent and Van der Werf (2014) is shown for two wave lengths (deep water and local depth). Using the deep water wave length, the rock size is about 20% larger. Equation (2.4.1) of Van Rijn is applied with $\alpha=2$, r=0.5, $\gamma_s=1$ (no safety factor) and $\gamma_{str}=1.5$ (to include effects of breaking, up and downrush and reflecting waves). As Equation (2.4.1) is related to the peak orbital velocity, the rock size decreases markedly for increasing water depth at the toe. The rock size increases by about 20% if a longshore current of 1 m/s is present (Equation 2.5.1 of Van Rijn). Equations (2.4.2) and (2.4.3) are only weakly related to water depth and cannot take the longshore current effect into account. All equations yield very similar results (rock sizes of 0.3 to 0.4 m) for worst-case conditions with breaking waves ($H_{s,toe}/h_{toe}\cong$ 0.5 to 0.6).
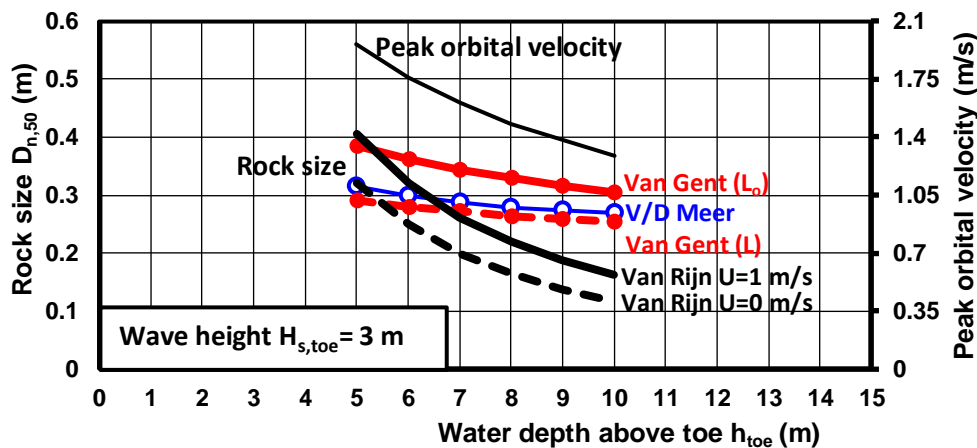

Figure 2.4.4 *Rock size of toe protections*

2.4.5 Practical application cobble revetment

A cobble revetment may be an effective solution to protect the upper beach and dune toe against wave attack and erosion (Komar and Allan 2010). A cobble revetment consisting of cobbles with sizes in the range of 0.05 to 0.25 m ($d_{n,50}\cong$ 0.15 m) has a more natural appearance compared to a conventional riprap revetment.
Using this approach, a dynamic revetment consisting loose, movable cobbles is obtained in contrast to a conventional static riprap revetment built of large quarry stones.
Stone sizes are significantly smaller (and cheaper) than required for armour sizes in a riprap revetment and construction is simpler than that of a conventional revetment resulting in a significantly cheaper solution.
The design slope of the revetment can be relatively steep (say 1 to 10), but the actual slope will be sorted out by the wave climate transporting the cobbles up and down the upper beach resulting in a dynamic equilibrium cobble slope. The thickness of the cobble layer (at least $10d_{n,50}$) should be sufficient to allow this sorting process to take place. If necessary, the cobble layer can be extended to the crest of the dune/dike.
The design of the cobble layer (with $d_{n,50}\cong0.15$ m) can be, as follows:
- cobble layer with thickness of 2 to 3 m and slope of 1 to 7 between the seabed at -4 m below MSL up to the dune/dike toe at +3 m above MSL (Mean Sea Level);
- cobble layer with thickness of 2 to 3 m and slope of 1 to 5 between +3 m and +10 m covering the dike/dune front;
- toe protection of rocks with sizes of 0.4 to 0.5 m at -4 m below MSL.

Based on this design, the total length of the cobble layer is about 7x7+5x7$\cong$85 m and the cobble volume is about 85x3$\cong$250 m^3/m or about 0.6x250/(π/6 x0.15^3)$\cong$85,000 cobbles/m.

Equations (2.4.1) and (2.3.3b) have been used to estimate the the number of moving cobbles per day under various conditions, see **Table 2.4.2**.

The input data are: $D_{n,50}$=0.15 m, slope 1 to 7; sea water density=1020 kg/m³; peak orbital velocities of 2, 2.5, 3 and 3.5 m/s; peak wave period T_p=10 s.

Cobbles are fairly stable in storm conditions with peak orbital velocities (or uprush and downrush velocities) of about 2.5 m/s. Considerable damage occurs if the peak velocities are approaching 3 m/s and failure occurs for peak velocities of about 3.5 m/s.

Peak orbital velocity (m/s)	Number of moving rocks per m and day (Number of available rocks≅85000 per m)
2	0.015
2.5	170
3.0	7800
3.5	55000

Table 2.4.2 *Damage of cobble beach protection*

Figure 2.4.5 *Cobble beach protection (Komar and Allan 2010)*

2.5 Stability and damage equations for coarse materials in currents plus waves

2.5.1 Equations

Using the available formulae (2.2.3, 2.2.4 and 2.2.5), the critical diameter can be expressed as:

$$D_{n,50} = \frac{\tau_{b,cw}}{(\rho_s - \rho_w) \, g \, (K_{\alpha 1} \, K_{\alpha 2} \, r \, \theta_{cr,o})} \tag{2.5.1}$$

with: $\tau_{b,cw}$ = shear stress at granular material due to currents plus waves (see Equation (2.2.4))
Equation (2.5.1) can be expressed as:

$$D_{n,50} = \frac{\gamma_s \, [0.013 \, (h/\alpha)^{-0.3} \, (\gamma_{str} \, \overline{u})^2 + 0.045 \, (T_p/\alpha)^{-0.3} \, (\gamma_{str} \, \hat{U})^{1.7}]^{1.4}}{[(s-1) \, g \, K_{\alpha 1} \, K_{\alpha 2} \, r \, \theta_{cr,shields}]^{1.4}} \tag{2.5.2}$$

r   = Shields-reduction coefficient= 0.4-1 (larger r-value yields smaller diameter);

α = bed roughness coefficient ($k_s=\alpha D_{n,50}$ with α=1.3 to 2); γ_s = safety factor;

γ_{str} = velocity+turbulence enhancement factor due to the presence of structures such as bridge piles or windmill piles (γ_{str}= 1 to 1.5; γ_{str} =1 if no structure is present).

s   = ρ_s/ρ_w, $K_{\alpha 1}$ = slope factor for longitudinal slopes, $K_{\alpha 2}$ = slope factor for lateral slopes,

$\theta_{cr,shields}$= critical Shields mobility parameter based on Equation 2.2.3; ($\theta_{cr,shields} \cong 0.05$ for coarse materials),

Equation (2.5.2) is implemented in the **ARMOUR.xls** model. Equations (2.3.3b) can be used to get an estimate of the number of moving rocks (damage) during a given period (used in **ARMOUR.xls**).
The damage parameter S_d can be estimated by:

$S_d=A_e/(D_{n,50})^2= \Delta t\, N_{movingrocks}\, V_{1rock}/(D_{n,50})^2= 0.5\, \Delta t\, N_{movingrocks}\, (\pi/6)\, (D_{n,50})^3/(D_{n,50})^2 \cong 0.5\, \Delta t\, N_{movingrocks}\, D_{n,50}$

with: A_e= eroded area per unit width in a given time period Δt, V_{1rock} = volume of single rock; Δt= time period considered (usually 5000 to 10000 waves or about 1 day of storm) and $N_{movingrocks}$ = number of moving rocks per m width and second based on Equation (2.3.3b).

2.5.2 Practical application of rock bed protection near monopiles

Bed protections around monopiles of wind mills in coastal waters are intensively studied. Equation (2.5.1) can be used to design the rock size of bed protection around the monoplile (see **Figure 2.5.2**) provided that the effect of the structure on the local velocity field is known with sufficient accuracy. This effect is represented by the γ_{str}-coefficient (range of 1 to 1.5) of Equation (2.5.1).
Miles et al. (2017) have studied the current and wave fields around a monopile at a scale of 1 to 25 in a wave-current basin. The waves are normal to the current. Based on their measured data, it can be concluded that:
- the most significant current-related wake region downstream of the pile has a length of 5D; the total distance of disturbed velocities is about 10D; the maximum turbulent velocities do occur at a distance of 2D downstream of the pile centre; the maximum standard deviation of the instantaneous velocities at that location is about $\sigma_U=0.7U_{c,o}$ with $U_{c,o}$= current velocity upstream of pile;
- the maximum velocity at both sides of the pile is about $U_{c,local}=1.35U_{c,o}$ at 0.75D from the pile centre (normal to main current direction);
- the wave-related influence zone with disturbed orbital velocities is about 3D on both sides of the pile (waves only); the maximum orbital velocity in the influence zone is about $U_{w,local}=1.85U_{w,o}$ with $U_{w,o}$= (undisturbed) near-bed orbital velocity outside influence zone.

De Vos et al. (2012) have performed experimental work (in a wave-current basin) on circular bed protections around a monopile foundation (windmill pile). The overall diameter of the circular bed protection is about $5D_{pile}$ with D_{pile}=pile diameter. The thickness of the bed protection is 2.5 to $3D_{n,50}$. Various sizes of angular protection material (sediment density of 2650 kg/m^3) have been used: $D_{n,50}$= 3.5, 5 and 7.2 mm. The protection material was placed on top of the sand bed (D_{50}= 0.1 mm).
Ten test results (**Table 2.5.1**) have been used to calibrate the γ_{str}-parameter of Equation (2.5.1) using: s=2.6, δ_{bp}=0.02 m= thickness protection layer, α=2, r=0.5, $\theta_{cr,shields}$=0.05, and γ_s=1 (safety factor). The γ_{str}-parameter represents the effect of the monopile on the enhancement of the local depth-mean velocity and the additional turbulence generated by the pile structure. The results are shown in **Table 2.5.1** (last two columns). The computed γ_{str}-values vary in the range 1.1 to 1.8 or γ_{str} =1.4±0.3 (about 20% variation). Miles et al. (2017) have found that the local velocity increase due to the presence of the pile is about 35%, which is in agreement with a velocity enhancement coefficient of γ_{str} =1.4.
The construction of a monopile in the seabed requires the protection of the local bed around the pile by a cover stone layer, see **Figure 2.5.2**. Often, the protection layer consists of a foundation layer and a cover layer. The length of the foundation layer is determined by the acceptable scour depth. The scour depth is of the order of $d_{s,max} \cong D_{pile}$ for $L_{foundation}=3D_{pile}$ and $d_{s,max} \cong 0.1D_{pile}$ for $L_{foundation}=6D_{pile}$ (Whitehouse et al. 2008).

Test	Stone size	Number of waves	Water depth	Depth-mean velocity u_{mean}	Significant wave height H_s	Peak wave period T_p	Dimensionless parameter related to scour of stones S_{3d}	Computed	
								γ_{str}	S_{damage}
	(mm)	(-)	(m)	(m/s)	(m)	(s)	(-)	(-)	(-)
6	3.5	5000	0.4	0.08	0.135	1.42	0.60; D.L.=3	1.2	<0.1
14	3.5	5000	0.4	0.164	0.088	1.42	0.24; D.L.=1	1.6	<0.1
19	3.5	3000	0.4	0.163	0.130	1.71	0.94; D.L.=3	1.1	<0.1
50	5.0	5000	0.4	0.224	0.109	1.71	0.64; D.L.=3	1.4	<0.1
52	5.0	3000	0.4	0.315	0.058	1.71	1.21; D.L.=4	1.6	<0.1
53	7.2	5000	0.4	0.156	0.145	1.71	0.35; D.L.=2	1.4	<0.1
54	7.2	5000	0.4	0.221	0.121	1.42	0.19; D.L.=2	1.6	<0.1
73	7.2	3000	0.4	0.066	0.151	1.71	0.98; D.L.=3	1.4	<0.1
77	7.2	3000	0.4	0.203	0.122	1.42	0.99; D.L.=3	1.6	<0.1
84	5.0	3000	0.4	0.214	0.135	1.42	0.40; D.L.=2	1.3	<0.1

D.L.=Damage Level; D.L.=2= very limited movement of stones (S_{3d}=0.3-0.5); D.L.=3 (S_{3d}=0.5-1)
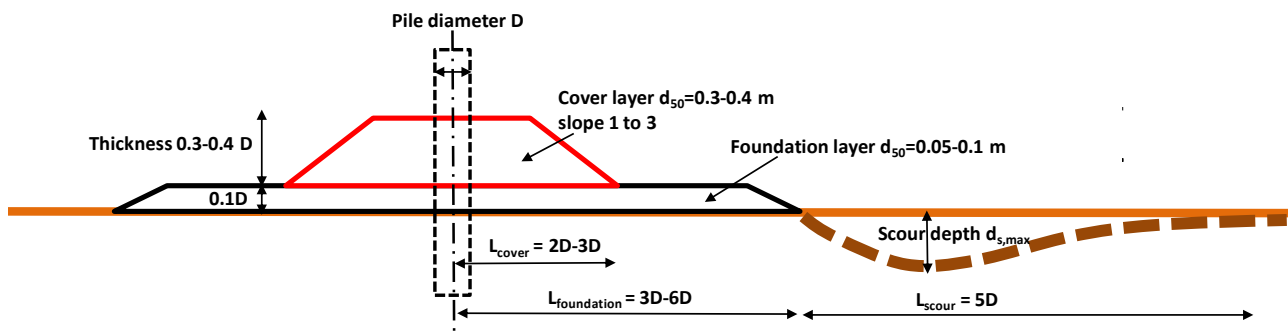**Table 2.5.1** *Stability test results of circular bed protections around a monopile*

Figure 2.5.2 *Bed protection layers around monopile*

De Vos et al. (2012) have defined a field example case with the following values: D_{pile}= 5 m, water depth h= 20 m, current U_{mean}= 1.5 m/s, significant wave height H_s= 6.5 m, peak wave period T_p= 11.2 s, density seawater ρ_w=1020 kg/m^3, thickness of protection layer δ_{bp}= 2 m.
The expression of the De Vos et al. (2012) yields: $D_{n,50}$= 0.34 m.
Equation (2.5.1) has also been used for this example. Using: effective water depth $h_{bp}=h_o-\delta_{bp}$=20-2=18 m, r= 0.5, $\theta_{cr,shields}$= 0.05 and α= 2, the rock size is: $D_{n,50}$= 0.34 m and $N_{moving\ rocks}$= 0.54 moving rocks/m/day ($S_d \cong 0.1$) for γ_{str}= 1.4. Thus, Equation (2.5.1) yields the same result as that of De Vos et al.

2.5.3 Practical application of rock bed protection near quay mooring

Traditionally, armour layers of rocks have been used for berth protection, but the required rock size now often makes it impractical and other scour protection solutions are required.
The size of conventional vessels (draughts up to 15 m; propeller diameters ranging from 4 to 8 m) is continually increasing creating propeller jet flows with higher velocities, while the bottom clearances are also reduced. The combination of larger propeller jet flows and a reduction in bed clearance has created higher levels of bed impact. In addition, propeller suction loads are also important. Transverse thrusters also known

as bow and stern thrusters (with diameters ranging from 1 to 3 m) are used to aid berthing and unberthing. Transverse thruster action onto quay walls can cause significant erosion from deflected downwash.

The berthing and unberthing actions for larger vessels will often be tug assisted. When twin tugs are used, the vessel propeller and transverse thrusters are usually not used, giving a low level of scour action upon a berth as tugs have a relatively large clearance. When one tug is used, the transverse thrusters of the ship are also needed for berthing.

The water jets of fast ferries have often caused significant erosion and damage to berths. During berthing, the high speed propulsion water jets with exit velocities in the range of 10 to 15 m/s are deflected under the vessel and cause direct scour of the bed. The most significant scour velocities for conventional vessels are produced when the vessel is near stationary and typically when unberthing.

Typical near-bed water velocities generated by ship propeller systems are (Hawkswood et al, 2014):

Propellers: 3 to 8 m/s,
Transverse thrusters: 2 to 4 m/s,
Water jets: 4 to 12 m/s.

Berth scour protection is often required to protect quay structures from the effects of berth scour actions. Slopes to piled jetties also need to be protected.

Rock protections generally consist of two layers ($2D_{n,50}$) of rip rap armour units upon a bedding/filter layer and geotextile filter material, see **Figure 2.5.4**. The width of the protection should about 5 to 10 m beyond the propelller axis to prevent/reduce scour at the outer edge of the protection layer. Rock protection often needs to be grouted at the quay walls to prevent wash out from flow down or along walls.

Figure 2.5.3 shows the rock diameter as function of the propeller-induced near-bed velocity based on research of BAW (2005). Rock diameters larger than 1 m are required for velocities > 4 m/s, which is often impractical. Large rock diameters lead to an increase of the span and embedment heights of the quay walls with major cost increase effects.

In conditions with large propeller-induced velocities, it may be more cost effective to use mattress or grouted rock systems. The failure mode of these systems generally is suction uplift.

Gabion mattresses are generally preformed from steel wire baskets containing rocks. These are generally prefilled and lifting into place for berth beds guided by divers and placed onto a filter fabric. Closed joints are required.

Equation (2.5.1) has also been used to estimate the stable rock size against near-bed velocities generated by ship propellers. it is assumed that the propeller axis is about 3 to 5 m above the bottom and that a boundary layer flow (with h=3 to 5 m) is generated locally.

The input parameters are: boundary layer height h=3 and 5 m, mean flow velocity in boundary layer u=2 to 6 m/s, bed roughness coefficient α=0.5, Shields reduction coefficient r= 0.5, Shields mobility number $\theta_{cr,shields}$= 0.05, turbulence enhancement factor γ_{str}=1.2. The computed results are plotted in **Figure 2.5.3** and are in reasonable agreement with the BAW-results. These computation results confirm that excessively large rock diameters are required to obtain stable rocks in conditions with velocities > 4 m/s close to the bottom.
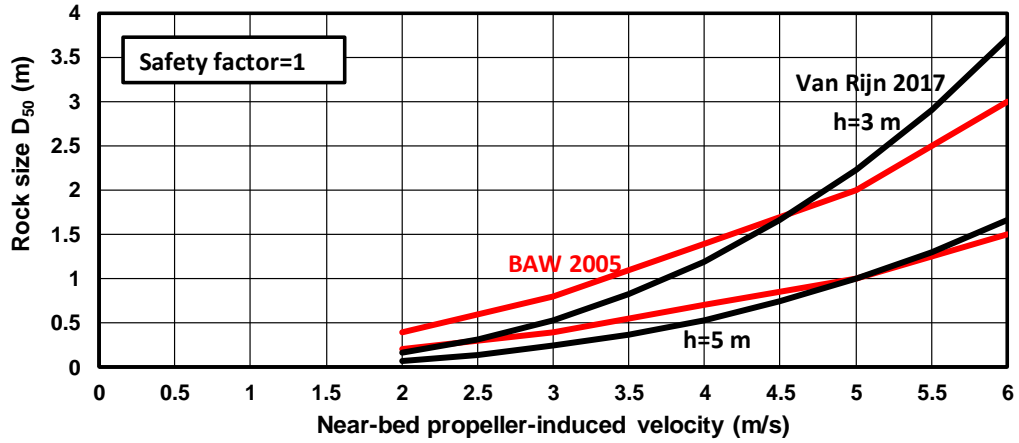
Figure 2.5.3 *Rock size for bed protection layers at berthing sites*
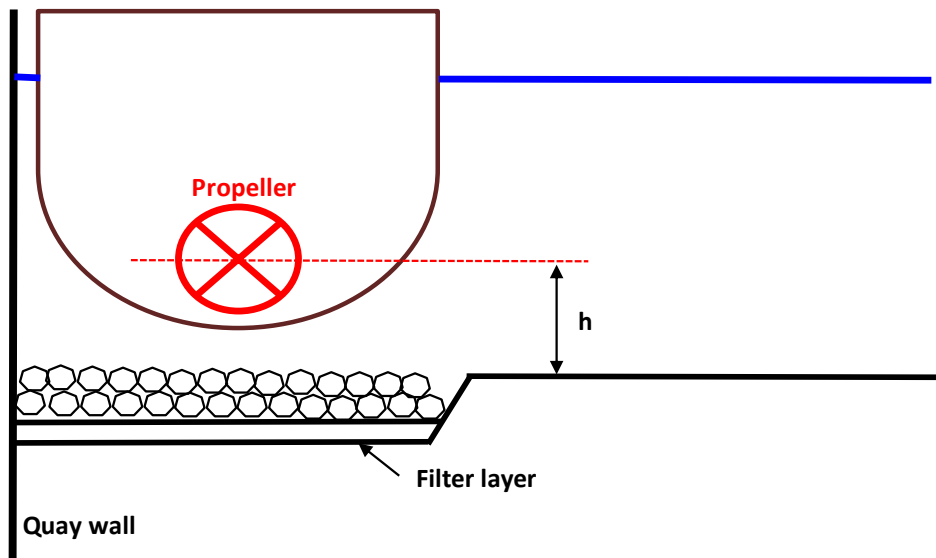
Figure 2.5.4 *Berth protection of rocks*

3.   Bed load transport of rocks

3.1   General

The transport of large cobbles, boulders and rocks is studied based on measured field and flume data. Various formulae are compared to the available data.

3.2   Measured bed load transport of cobbles, boulders and rocks

3.2.1 Flume data

__Data of Meyer-Peter-Mueller 1948__
A subset of the flume data of Meyer-Peter-Mueller (1948) has been analyzed and plotted in **Figure 3.2.1**. The data are given in **Table 3.2.1**. The particle sizes are D_{50}=28 mm and 5.2 mm. The water depths vary in the range of 0.06 m in the narrow flume (width=0.35 m) up to 1.09 m in the wide flume (width=2 m). The cross-section-averaged velocities are in the range of 0.85 to 2.85 m/s.
Figure 3.2.1 shows the dimensionless bed load transport rate ϕ_b as function of the grain-related Shields parameter θ.
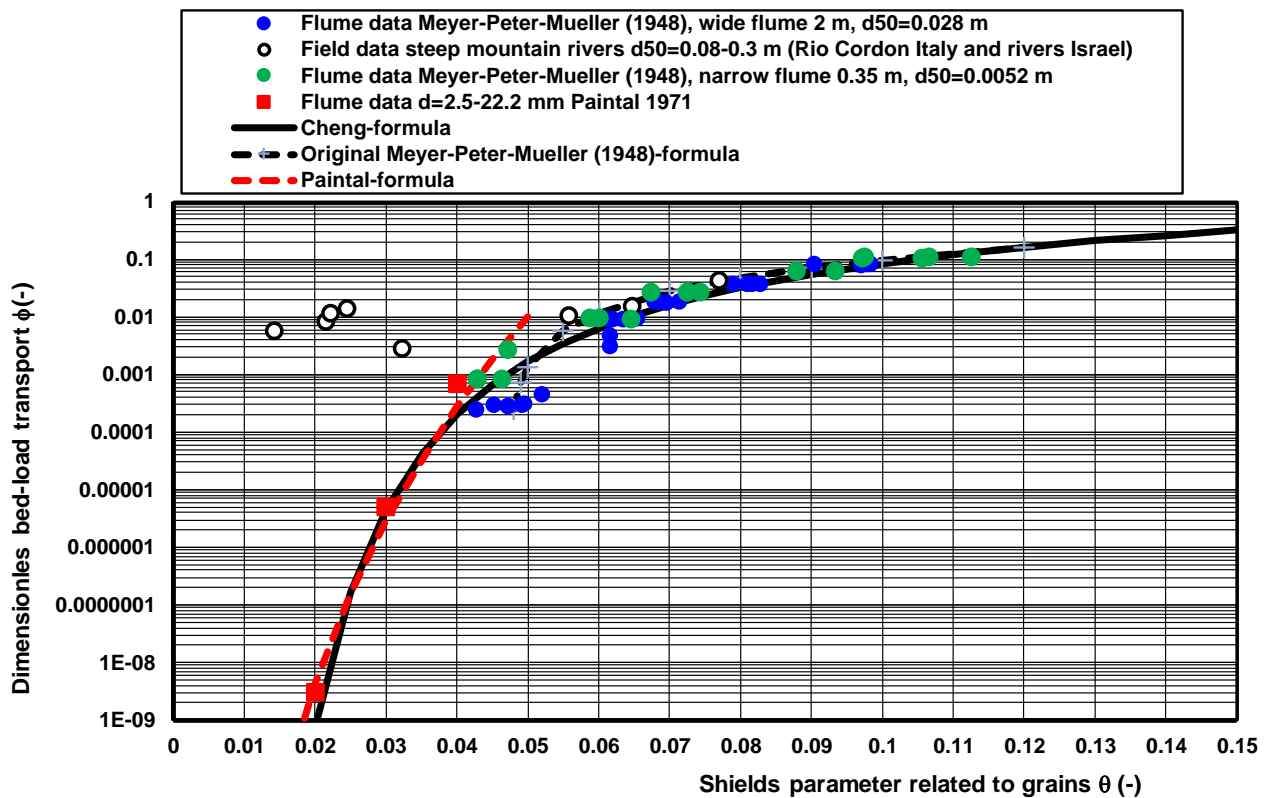
Figure 3.2.1   *Dimensionless bed load transport at low values of the Shields parameter*

	Flume data MPM	1948						
	Discharge	Width	Depth	Slope	d50	Gradation	Concentration	Bedload tr.
	(m3/s)	(m)	(m)	(-)	(mm)	(-)	(ppm)	(kg/s)
1	1.64	2	0.39	0.0107	0.0287	1	1105	1.8122
2	1.64	2	0.44	0.0065	0.0287	1	29	0.04756
3	1.64	2	0.4	0.0092	0.0287	1	603	0.98892
4	1.64	2	0.4	0.00927	0.0287	1	598	0.98072
5	1.64	2	0.4	0.0092	0.0287	1	596	0.97744
6	1.64	2	0.4	0.00914	0.0287	1	617	1.01188
7	1.64	2	0.4	0.00915	0.0287	1	603	0.98892
8	1.64	2	0.37	0.0137	0.0287	1	2333	3.82612
9	1.64	2	0.41	0.0082	0.0287	1	303	0.49692
10	1.64	2	0.41	0.0076	0.0287	1	194	0.31816
11	1.64	2	0.45	0.0056	0.0287	1	19	0.03116
12	1.64	2	0.34	0.0176	0.0287	1	5103	8.36892
13	3.27	2	0.6	0.0122	0.0287	1	2589	8.46603
14	3.27	2	0.65	0.0085	0.0287	1	1175	3.84225
15	3.27	2	0.7	0.0071	0.0287	1	585	1.91295
16	3.27	2	0.72	0.0059	0.0287	1	295	0.96465
17	3.27	2	0.73	0.0058	0.0287	1	295	0.96465
18	3.27	2	0.83	0.0035	0.0287	1	9.6	0.031392
19	3.27	2	0.85	0.0034	0.0287	1	8	0.02616
20	3.27	2	0.6	0.0124	0.0287	1	2589	8.46603
21	4.61	2	0.8	0.0109	0.0287	1	1829	8.43169
22	4.48	2	0.78	0.0107	0.0287	1	1896	8.49408
23	4.58	2	0.86	0.0074	0.0287	1	834	3.81972
24	4.55	2	0.85	0.0074	0.0287	1	834	3.7947
25	4.58	2	0.91	0.0058	0.0287	1	421	1.92818
26	4.6	2	0.93	0.0058	0.0287	1	416	1.9136
27	4.6	2	0.97	0.0048	0.0287	1	208	0.9568
28	4.6	2	0.96	0.005	0.0287	1	207	0.9522
29	4.6	2	1.09	0.0032	0.0287	1	6.4	0.02944
30	4.6	2	1.09	0.0032	0.0287	1	6.4	0.02944
31	1.64	2	0.35	0.0176	0.0287	1	5171	8.48044
32	3.37	2	0.82	0.0039	0.0287	1	9.6	0.032352
33	0.0217	0.354	0.06	0.0227	0.0052	1	6896	0.1496432
34	0.0217	0.354	0.071	0.00964	0.0052	1	598	0.0129766
35	0.0217	0.354	0.067	0.0126	0.0052	1	1743	0.0378231
36	0.0217	0.354	0.061	0.0176	0.0052	1	4085	0.0886445
37	0.0217	0.354	0.058	0.0222	0.0052	1	6999	0.1518783
38	0.0608	0.354	0.136	0.0112	0.0052	1	2536	0.1541888
39	0.0608	0.354	0.1475	0.0089	0.0052	1	1467	0.0891936
40	0.0608	0.354	0.16	0.0062	0.0052	1	631	0.0383648
41	0.0608	0.354	0.16	0.0063	0.0052	1	631	0.0383648
42	0.0608	0.354	0.175	0.0047	0.0052	1	223	0.0135584
43	0.0608	0.354	0.2	0.0032	0.0052	1	19.1	0.00116128
44	0.0608	0.354	0.2	0.0033	0.0052	1	19.1	0.00116128
45	0.0433	0.354	0.145	0.0037	0.0052	1	27.1	0.00117343
46	0.0433	0.354	0.1	0.0131	0.0052	1	3568	0.1544944
47	0.0433	0.354	0.13	0.0056	0.0052	1	312	0.0135096
48	0.0821	0.354	0.182	0.0098	0.0052	1	1883	0.1545943
49	0.0821	0.354	0.213	0.0054	0.0052	1	467	0.0383407
50	0.0821	0.354	0.248	0.0032	0.0052	1	46.3	0.00380123

Table 3.2.1 *Flume data of Meyer-Peter-Mueller (1948); d_{50}=0.028mm and 0.0052 m*

Paintal data (1971)

An important contribution to the study of the stability of granular material has been made by Paintal (1971), who has measured the dimensionless (bed load) transport of granular material at conditions with θ-values in in the range of 0.01 to 0.04, see **Figure 3.2.2** and **Table 3.2.2**.

The results of Paintal can be represented by:

$$\Phi_b = 6.6 \ 10^{18} \ \theta^{16} \tag{3.2.1}$$

with:

Φ_b $= (\rho_s)^{-1} \{(s-1)g\}^{-0.5} (D_{50})^{-1.5} q_b$;

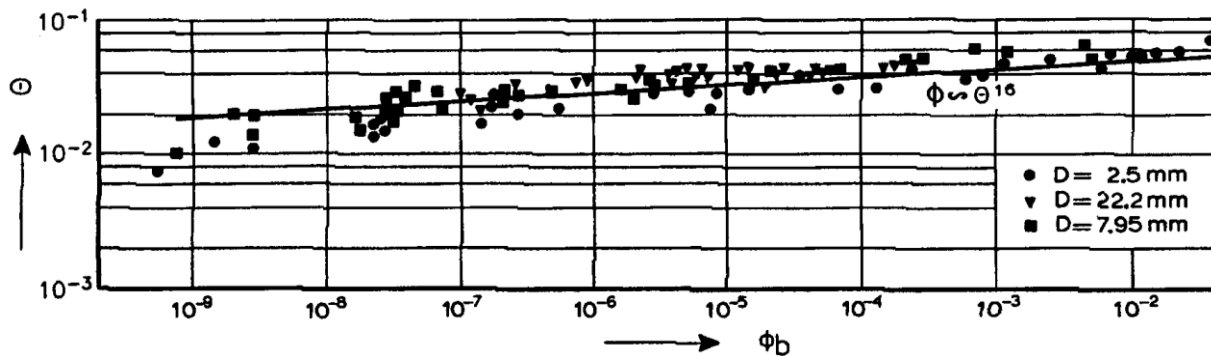q_b $=$ bed load transport by mass (kg/m/s);

θ $= \tau_b/[(\rho_s - \rho_w) g D_{50}] =$ dimensionless bed-shear stress (Shields number);

s $= \rho_s/\rho_w =$ relative density;

τ_b $=$ bed-shear stress due to current (N/m^2).

θ-values	Dimensionless bed load transport Φ measured by Paintal (1971)
0.01	$4.3 \ 10^{-11}$
0.02	$4.3 \ 10^{-9}$
0.025	$1.5 \ 10^{-7}$
0.03	$3. \ 10^{-6}$
0.04	$3. \ 10^{-4}$

Table 3.2.2 *Bed load transport measured by Paintal (1971)*

Figure 3.2.2 *Dimensionless bed load transport according to Paintal (1971)*

3.2.2 Field data

Rio Cordon, Italy

The research was conducted in the Rio Cordon catchment (5 km^2), a small mountain stream in the Dolomites located in the eastern Italian Alps (Lenzi 2004, Lenzi et al. 2006, Mao and Lenzi 2007, Rainato etal. 2017). The main channel (13.6% as mean gradient) features cascade and step-pool reaches. The sediment characteristics are: D_{10}=26 mm, D_{50}=120 mm and D_{90}=450 mm. The ratio D_{50}/D_{90}=0.26 (wide graded mixture). The channel width during flood, in a typical cross-section just upstream of the station, varies from 5 to 7 m, depending on the discharge. The measuring station consists of an inlet flume, an inclined grid where the separation of coarse particles takes place, a storage area for coarse sediment deposition, and an outlet flume to return water and fine sediment to the stream (**Figure 3.2.3**).

An exceptional flood event occurred on 14 September 1994, see **Table 3.2.3**. The mean flow velocity was about 3 m/s and the measured bed load transport was about 14 kg/m/s. Assuming that the rock transport

velocity is about 1.5 m/s (50% of flow velocity), the bed load is about 10 kg/m^2 which is equivalent to 7 moving rocks per m^2 (about 10% of bed surface is moving).

Parameter	Value
Rock/rock diameter	0.1 m
Mass of 1 rock	1.4 kg
Water discharge	10.4 m^3/s
Flow width (estimated) (measured flow width= 5 m at discharge of 2.3 m^3/s)	7 m
Water depth (estimated)	0.5 m
Flow velocity (estimated)	10.4/(7x0.5)= 3 m/s
Effective grian roughness (estimated)	2d$_{50}$= 0.2 m
Bed-shear stress (estimated) Critical bed-shear stress	120-150 N/m^2 100 N/m^2
Estimated mobility number (θ)	0.074-0.093
Particle velocity $\cong$ 0.5 flow velocity	= 1.5 m/s
Bed load transport= load x particle velocity	225 m^3/hour= 0.009 m^3/m/s = 14 kg/m/s = 10 rocks/m/s
Load= bed load transport/particle velocity	$\cong$14/1.5 $\cong$ 10 kg/m^2 $\cong$ 7 rocks per m^2 $\cong$ 10% of bed surface is moving

Table 3.2.3   *Bed load transport data of flood event 14 September 1994, Rio Cordon, Italy*

Figure 3.2.3   *Measuring station Rio Cordon, Italy*

Jordan and Meshushim Rivers, Israel

Inbar and Schick (1979) have studied bed load transport during flash floods in the upper Jordan River and the Meshushim River in Israel. The Jordan River drains an area of 1590 km^2 into Lake Kinneret. Rainfall (rain storms) is only present in winter. Peak flow approximates 100 m^3/s. The highest flow during the 43 years recorded is 214 m^3/s. Bedload transport is about 1% to 2% of the total sediment yield and occurs mainly during flows that exceed 60 m^3/s (flow velocity of 1.5 m/s).

Before entering Lake Kinneret, the Jordan River flows in a narrow and deep canyon entrenched in basalt. The canyon section is 10 km long and represents a 240 m drop in riverbed elevation. The study reported here was

made in the alluvial section of the river located between the canyon outlet and Lake Kinneret, a reach 4 km long.

An extreme rainstorm (once in 100 years) in January 1969 generated a flood in the Jordan River. Boulders up to 1.3 m were moved, and the channel was completely reshaped. During the same event, a 300 m^3/s peak flow occurred in the neighboring Nahal Meshushim, which drains 160 km^2 of basaltic terrain in the Golan Heights into Lake Kinneret just east of the Jordan outlet. Here too, numerous boulders of 1 m were transported.

The braided channel area of the Jordan River is composed mainly of boulders, rocks, and pebbles larger than 32 mm. Boulders of 1 m moved only once during recent decades, when the January 1969 flood exceeded a peak discharge of 200 m^3/s and the mean velocity was 3 to 4 m/s.

At discharges of 100 m^3/s (flow velocity $\cong$ 2.5 m/s), about 6% of the available boulders in the size class of 0.5-1 m and 12% of size 0.25-0.5 m moved. No coarse bedload moved at discharge values below 60 m^3/s (velocity $\cong$ 1.5 m/s). In the Meshushim river, boulders of 0.25-0.5 m did move but boulders of 0.5 m did not move during events with discharges of 50-80 m^3/s (1.5 to 2 m/s).

River	Date and event duration (hours)	Boulder diameter (m)	Discharge (m³/s)	Width (m)	Depth (m)	Slope (-)	Mean velocity (m/s)	Mobility number (-)	Bed load transport (kg/m/s)
Jordan	22-25 Jan. 1969 (72 hrs)	0.3	180-214	43	1.4	0.035	3.3	0.032	3.0x1.6=4.8
	21 Jan. 1974 (10 hours)	0.1	91-98	40	1.2	0.035	2.0	0.022	1.7x1.6=2.7
	21 Jan. 1974 (10 hours)	0.1	91-98	24	1.7	0.03	2.3	0.024	2.8x1.6=4.5
	10 Feb. 1975 (6 hours)	0.08	55-60	34	1.1	0.035	1.5	0.014	0.8x1.6=1.3
	10 Feb. 1975 (6 hours)	0.08	55-60	19	1.5	0.03	2.0	0.022	1.7x1.6=2.7
Meshushim	22 Jan. 1969 (3 hours)	0.3	300	31	2.0	0.03	4.8	0.056	11x1.6=17.6
	22 Jan. 1969 (10 hours)	0.2	200	26	1.7	0.03	4.5	0.065	8.6x1.6=13.8

Bed load is given as immersed weight, which can be converted to weight by multiplying with $\rho_s/(\rho_s-\rho) \cong 1.6$
Effective grain roughness $k_s=2d_{50}$

Table 3.2.4 *Bed load transport data of Jordan and Meshushim rivers (Israel)*

The critical flow velocities in depths of 1 to 1.5 m can be summarized, as follows:
D_{50}= 0.25-0.5 m: $u_{critical}$= 2-2.5 m/s,
D_{50}= 0.5-1 m: $u_{critical}$= 2.5-3 m/s.

Table 3.2.4 shows the characteristic data of various flash flood events. The measured bed load transport data are shown in **Figure 3.2.1**.

3.2.3 Summary of flume and field data

Figure 3.2.1 shows the dimensionless bed load transport as function of the dimensionless grain-related Shields parameter for the available flume and field data. The grain roughness is set to k_s=1.5 d_{50} for the flume data and k_s=2d_{50} for the field data (relatively wide grading).

The following trends can be observed:
- all bed load transport data (blue and green dots) of MPM have a Shields parameter θ>0.04;
- the field bed load transport data are in good agreement with the data of MPM for Shields values between 0.05 and 0.08; four outliers with relatively high transport rates for low Shields values <0.03 are present, which may be caused by the transport of relatively fine sediments in the case of a very wide grain size distribution;
- the data scatter is relatively large around the critical Shields values of 0.01 to 0.05.

3.3 Bed load transport equations

3.3.1 Formulas used

The bed load transport equation of Meyer-Peter-Mueller (1948) reads, as:

$$\Phi_b = 8 \ (\theta - \theta_{cr})^{1.5} \tag{3.3.1}$$

The dimensionless parameters are defined as:
ϕ_b= q_b/[$\rho_s \, g^{0.5} \, (s-1)^{0.5} \, D_{50}^{1.5}$]= dimensionless bed load transport;
$\theta = \tau_b'/[(\rho_s-\rho_w) \, g \, D_{50}]$= dimensionless mobility parameter (Shields parameter);
θ_{cr}= critical Shields parameter= 0.047 (-);
q_b= bed load transport (kg/m/s);
ρ_s= sediment density (2650 kg/m^3),
ρ= fluid density (1000 kg/m^3),
s= ρ_s/ρ_w= relative density (-);
D_{50}= grain (rock) diameter (m);
τ_b= 0.125 $\rho_w f_c$ [U_{mean}]^2= bed-shear stress (N/m^2),
U_{mean}= depth-mean velocity (m/s);
f_c= 0.11 (h/αD_{50})$^{-0.3}$ =grain-related friction coefficient (-),
h= water depth (m),
α=coefficient ($\cong$1.5 to 2).
The original MPM-equation is valid for θ_{cr}= 0.047 and is shown in **Figure 3.2.1**.

The bed-load transport equation of Cheng (2002) can also be used for very coarse materials. This equation reads as:

$$\Phi_b = 13 \ \theta^{1.5} \exp(-0.05/\theta^{1.5}) \tag{3.3.2a}$$
$$q_b = 13\theta^{1.5}\exp(-0.05/\theta^{1.5}) \ \rho_s \ [(s-1)g]^{0.5} \ (D_{50})^{1.5} \tag{3.3.2b}$$

Equation (3.3.2) is shown in **Figure 3.2.1**.
Equation (3.3.2) has no threshold value. At high θ-values, the bed load transport approaches to
$\Phi_b = 13 \ \theta^{1.5}$.

The original MPM-equation shows good agreement with the MPM-flume data for α=1.5, which means that the effective grain roughness of the coarse sediment bed in the MPM-flumes can be represented by k_s= 1.5 D_{50}. The original MPM equation shows good agreement with the field data for θ-values in the range of 0.06 to 0.08.

The computed bed load transport rates based on the deterministic formula of MPM are zero for $\theta < \theta_{cr}$, whereas the measured transport rates in field conditions are non-zero for $\theta < 0.03$. This implies that the deterministic approach of MPM fails for conditions around the threshold conditions (θ_{cr}= 0.03 to 0.05).

The equation of Cheng shows fairly good agreement with the measured bed load transport rates of Paintal (1971).

The field data for $\theta<0.035$ are strongly underpredicted by both equations. Two explanations may be possible for this discrepancy. The measured bed load transport values which are derived from post flood deposits may have been "polluted" by the presence of much finer sediments transported as suspended load. It is known that steep coarse bed rivers generally have a very wide particle size distrution with $D_{90}/D_{10} \cong 20$ to 30 and thus a relatively large finer fraction. Furthermore, the depth-mean velocity may have been underestimated by the field workers during the flash flood event.

3.3.2 Bed load transport computations

Figure 3.3.1 shows the bed-load transport (in kg/m/s) for various rock sizes ($D_{n,50}$ = 0.05, 0.1, 0.2 and 0.3 m) based on Equations (3.3.1) and (3.3.2). The grain roughness is computed as k_s=1.5$D_{n,50}$.

It can be seen that the bed load transport of MPM is almost constant for diameters in the range of 0.05 to 0.3 m and velocities > 7 m/s. For example, the bed load transport of MPM is about 60 ($\pm$20) kg/m/s for a velocity of 7 m/s.
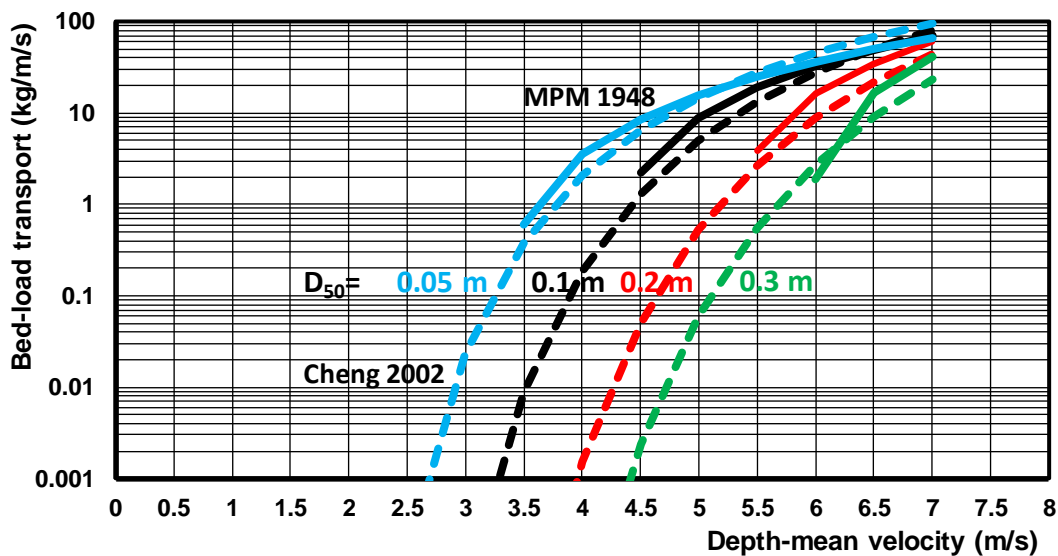

Figure 3.3.1 *Computed bed load transport (in kg/m/s) of MPM (1948) and Cheng (2002)*

4.   Conclusions

Cobbles, boulders and rocks are often used as a bed protection layer or armour layer near a structure to protect the underlying sand bed against erosion by combined currents and waves. The design of a bed protection layer consisting of loose rocks (rubble mound) requires knowledge of the stability and movement (as bed load) of very coarse materials. If some movement (or damage) is acceptable, the rock diameter can be designed to be smaller. This paper has addressed the stability and movement of very coarse materials (cobbles, boulders and rocks) based on the concept of the critical Shields mobility number related to a prescibed damage level. Universal equations for the design of rock sizes of bed protection layers (including damage) in conditions with currents with or without waves are proposed. The damage parameter is derived from the bed load equation of Cheng (2002), which is valid for relatively small Shields mobility numbers. The following conclusions are given:

1.   The sediment size of bed protection layers consisting of cobbles, boulders and rocks can be computed using the concept of the Shields mobility number, both in currents, waves and combined currents plus waves.
2.   The critical Shields number can be related to a prescribed damage level, which is expressed by the r-coefficient being a correction parameter in the range of r=0.4-0.5 to the original Shields'curve value of 0.05 for coarse materials. Smaller r-values yield larger rock sizes.
3.   The most realistic critical Shields number for stable coarse materials is $\theta_{cr} \cong 0.02$ to 0.025 (r= 0.4 to 0.5).
4.   The effect of the structure on the near-bed velocity and turbulence field can be taken into account by a velocity enhancement coefficient (γ_{str}), which has been found to be in the range of 1.1 to 1.7 (mean value of 1.4) for monopiles.
5.   The bed load transport of rocks with diameters of 0.1 to 0.5 m for Shields numbers > 0.05 can be very well described by the original Meyer-Peter-Mueller bed load transport equation.
6.   The bed load transport of rocks for Shields numbers in the range of $\theta= 0.01$ to 0.04 can be described by the equation Cheng (2002). This equation can be used to estimate the damage of a rock-type bed protection in extreme conditions.

5. References

Attal, M. and Lavé, J. 2009. Pebble abrasion during fluvial transport. Journal of Geophysical Research, Vol. 114

BAW, 2005. Principals for the Design of Bank and Bottom Protection for Inland waterways, Bulletin 85, Karlsruhe, Germany

Cheng, N.S., 2002. Exponential formula for bed load transport. Journal of Hydraulic Engineering, ASCE, Vol. 128, No. 10, 942-946.

CIRIA/CUR, 2007. Manual on the use of rock in coastal and shoreline engineering. Delft, The Netherlands

Crickmore, M.J., Waters, C.B. and Price, W.A. The measurement of offshore shingle movement. Proc. 13th ICCE, Vancouver, Canada

Deltares, 1972. Systematic investigation of two-dimensional and three-dimensional scour (in Dutch). Report M648/M893, Delft, The Netherlands

De Vos, L., De Rouck, J., Troch, P. and Frigaard, P., 2012. Empirical design of scour protections around monopile foundations, Part 2: Dynamic approach. Coastal Engineering Vol. 60, 486-498

Fahnestock, R.K. 1963. Morphology and hydrology of a glacial stream White River, Mount Rainier. U.S. Geological Survey Professional Paper 422-A, Washington, USA

Graf, W. H., 1971. Hydraulics of sediment transport. Mc Graw-Hill, New York, USA

Hall, A.M., 2010. Storm wave currents, boulder movement and shore platform development: a case study from East Lothian, Scotland. Marine Geology 283, 98-105

Hansom, J.D., Barltrop, N.D.P. and Hall, A.M., 2008. Modelling the processes of cliff-top erosion and deposition under extreme storm waves. Marine Geology 253, 36-50

Hawkswood, M.G, Lafeber, F.H. and Hawkswood, G.M., 2014. Berth scour protection for modern vessels. PIANC San Francisco, USA

Helley, E.J., 1969. Field measurement of the initiation of large bed particle motion in Blue Creek near Klamath, California. U.S. Geological Survey Professional Paper 562-G, Washington, USA

Hudson, R.Y., 1958. Design of quarry stone cover layers for rubble mound breakwaters. WES, Research Report No. 2-2, USA

Inbar, M. and Schick, A.P., 1979. Bed load transport associated with high stream power, Jordan River, Israel. Proc. National Academic Science, USA, Vol. 76, No. 6, 2525-2517

Komar, P.D. and Allan, J.C., 2010. "Design with Nature" strategies for shore protection—The construction of a cobble berm and artificial dune in an Oregon State Park, *in* Shipman, H., Dethier, M.N., Gelfenbaum, G., Fresh, K.L., and Dinicola, R.S., eds., 2010, Puget Sound Shorelines and the Impacts of Armoring—Proceedings of a State of the Science Workshop, May 2009: U.S. Geological Survey Scientific Investigations Report 2010-5254, 117-126.

Lenzi, M.A., 2004. Displacement and transport of marked pebbles, rocks and boulders during floods in a steep mountain stream. Hydrological processes, Vol. 18, No. 10, 1899-1914.

Lenzi, M.A., Mao, L. and Comiti, F., 2006. Effective discharge for sediment transport in a mountain river. Journal of Hydrology Vol. 326, 257-276

Mao, L. and Lenzi, M.A., 2007. Sediment mobility and bed load transport conditions in an alpine stream. Hydrological processes, Vol. 21, No. 10, 1882-1891

Meyer-Peter, E. and Mueller, R. 1948. Formulas for bed load transport. IAHR 2nd meeting, Stockholm, 41-64

Miles, J., Martin, T., and Goddard, L., 2017. Current and wave effects around wind farm monopile foundations. Coastal Engineering 121, 167-178

Mueller, E.R., Pitlick, J. and Nelson, J.M., 2005. The variation in the reference Shields stress for bed load transport in gravel-bed streams and rivers. Water Resources Research Vol. 41

Paintal, A.S., 1971. Concept of critical shear stress in loose boundary open channels. Journal of Hydraulic Research, Vol. 9, No. 1

Rainato, R. et al., 2017. Three decades of monitoring in the Rio Cordon instrumented basin:

Sediment budget and temporal trend of sediment yield. Geomorphology 291, 45-56

Schiereck, G.J. and Verhagen, H.J., 2016. Introduction to bed, bank and shore protection. Delft Academic Press, Delft, The Netherlands

Shields, A., 1936. Anwendung der Ähnlichkeitsmechanik und der Turbulenz Forschung auf die Geschiebebewegung. Mitt. der Preuss. Versuchsambt für Wasserbau und Schiffbau, Heft 26, Berlin

Soulsby, R. 1997. Dynamics of marine sands. Thomas Telford, UK

Turowski, J.M. et al., 2009. The impact of exceptional events on erosion, bedload transport and channel stability in a step-pool channel. Earth Surface Processes and Landforms Vol. 34, 1661-1673

Van der Meer, J.W., 1988. Rock slopes and gravel beaches under wave attack. Doctoral Thesis, Civil Engineering, Delft University of Technology, Delft, The Netherlands

Van der Meer, J.W., 1998. Geometrical design of concrete armour layers. Chapter 9 in: "Seawalls, dikes and revetments" edited by K.W. Pilarczyk. Balkema, Rotterdam, The Netherlands

Van Gent, M.R.A. and Van der Werf, I.M., 2014. Rock toe stability of rubble mound breakwaters. Coastal Engineering, Vol. 83, 166-176

Van Rijn, L.C., 1993, 2017. Principles of sediment transport in rivers, estuaries and coastal seas, Part I and II. Aquapublications. The Netherlands

Van Rijn, L.C. 2011. Principles of fluid flow and surface waves in rivers, estuaries, seas and oceans. Aquapublications, The Netherlands

Van Rijn, L.C., 2018. Erodibility of mud-sand bed mixtures (in preparation for Journal of Hydraulic Engineering, ASCE).

Whitehouse, R., Harris, J., Sutherland, J. and Rees, J., 2008. An assessment of field data for scour at offshore wind turbine foundations. Fourth International Conference on scour and erosion, Tokyo.

Yalin, M.S., 1977. Mechanics of sediment transport. Pergamon Press, Oxford